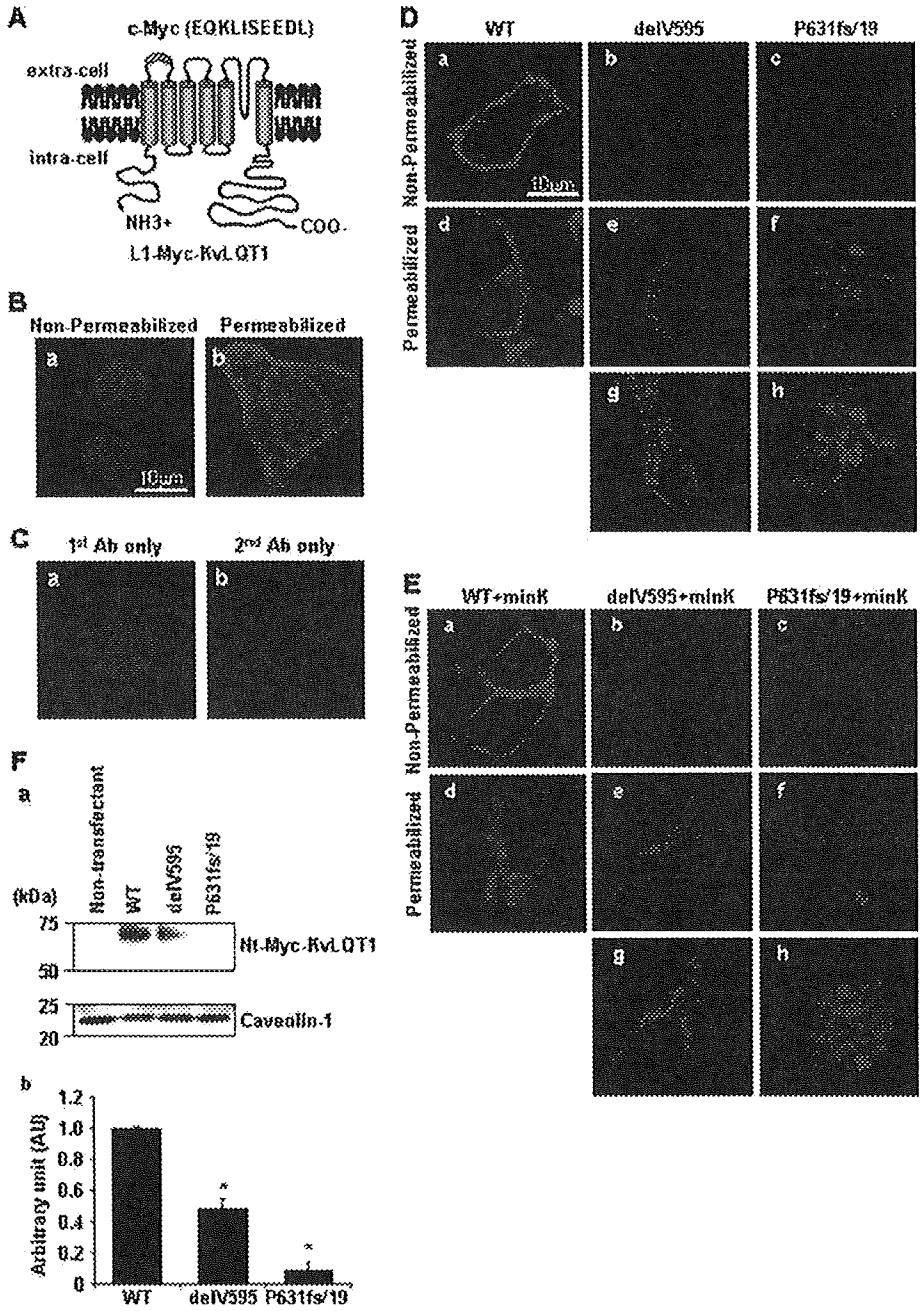

FIGURE 5. **Distribution of transiently expressed Myc-tagged KvLQT1.** *A*, schematic representation of the KvLQT1 channel containing the extracellular Myc epitope in the Linker 1 region between the membrane-spanning segments 1 and 2. *B*, HEK293 cells were fixed without (*a*; non-permeabilized condition) or with (*b*; permeabilized condition) 0.15% Triton X-100, respectively, and stained with anti-α-tubulin Ab (*red*) and 4′,6-diamidino-2-phenylindole (*blue*). *C*, HEK293 cells were fixed under the permeabilized condition and stained with only anti-c-Myc Ab without secondary Ab (*a*) or only secondary Ab without anti-c-Myc Ab (*b*) and 4′,6-diamidino-2-phenylindole (*blue*). *D* and *E*, HEK293 cells transfected with L1-Myc- KvLQT1-WT (*a* and *d*), -delV595 (*b*, *e*, and *g*), and -P631fs/19 (*c*, *f*, and *h*) in the absence (*D*) or presence (*E*) of MinK were fixed without (*a–c*; non-permeabilized condition) or with (*d–f*; permeabilized condition) 0.15% Triton X-100, respectively, and stained with anti-c-Myc Ab. *g* and *h*, highly sensitized images taken from *e* and *f*, respectively. Surface expression of each KvLQT1-mutant was impaired (*b* and *c*), and each mutant showed reduced fluorescence intensity (*e* and *f*) with abnormal granular distribution (*g* and *h*). *Scale bar*, 10 μm. *F*, expression of Myc-tagged KvLQT1 proteins in the membrane-enriched fraction obtained from non-transfectant, KvLQT1-WT-, KvLQT1-delV595-, and KvLQT1-P631fs/19-transfected HEK293 cells. *a*, *upper lanes*, detection of Nt-Myc-KvLQT1 proteins by anti-c-Myc Ab. *Lower lanes*, detection of caveolin-1 showing that the similar amounts of cell membrane protein were subjected to the Western blot analysis. *b*, densitometric data obtained from *a* are indicated as -fold expression relative to Nt-Myc-KvLQT1 normalized by caveolin-1 protein. The data for KvLQT1-WT were arbitrarily defined as 1.0. Data are represented as means ± S.E. ($n = 4$ for each case). *, $p < 0.001$ *versus* WT.

defect in the cytoplasm and found that there were R^{633}GR and R^{646}LR sequences (Fig. 8*A*). Because the *RXR* motif was acknowledged to be a retention signal to ER, we constructed three variants of L1-Myc-KvLQT1-P631fs/19 carrying A^{633}AA + R^{646}LR, R^{633}GR + A^{646}AA, or A^{633}AA + A^{646}AA (Fig. 8*A*) and tested for the trafficking. It was discovered that A^{633}AA + R^{646}LR and R^{633}GR + A^{646}AA did not suppress the defects (Fig. 8*B*, *panels c* and *h* and *panels d* and *i*), whereas A^{633}AA + A^{646}AA relieved the defects (Fig. 8*B*, *e* and *j*), suggesting that these *RXR* motifs were responsible for the trafficking defect.

Quantitative Analysis of Cell Surface Expression of KvLQT1 Channel Protein—To quantitatively investigate the cell surface expression of the KvLQT1 channel, we developed a luminometric analysis of the L1-Myc-tagged KvLQT1 (Fig. 9). As shown in Table 2, L1-Myc-KvLQT1-delV595, L1-Myc-KvLQT1-P631fs/19, and L1-Myc-KvLQT1-P631fs/19 carrying A^{633}AA + R^{646}LR, and -P631fs/19 carrying R^{633}GR + A^{646}AA, Nt-Myc-KvLQT1-WT, and Myc(−)-KvLQT1-WT showed significantly less expression on the cell surface than the L1-Myc-KvLQT1-WT ($p < 0.001$ in each case) On the other hand, L1-Myc-KvLQT1-P631stop, -P631fs2/34, and -P631fs/19 carrying A^{633}AA + A^{646}AA were expressed at a similar level as L1-Myc-KvLQT1-WT.

DISCUSSION

In the present study, we found two *KCNQ1* mutations, delV595 and P631fs/19, which caused LQTS without hearing loss in two compound heterozygotes (proband and affected brother). No significant QT elongation was observed in either heterozygote (father and mother), implying that both mutations lacked the dominant negative effect. As shown in Fig. 3, both mutants were non-functional by themselves, and the mutant channels lacked the dominant negative suppression properties, consistent with the clinical observations that the heterozy-

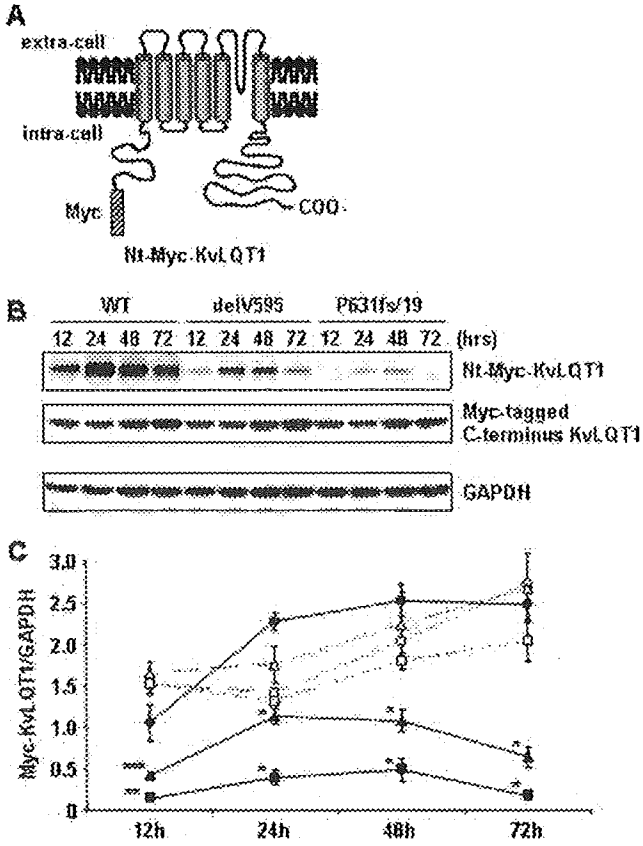

FIGURE 6. **Expression and stability of transiently expressed Myc-tagged KvLQT1.** *A*, schematic representation of the KvLQT1 channel tagged with Myc at the N-terminal cytoplasmic region. *B* (*top*), expression of Nt-Myc-KvLQT1-WT, -delV595, and -P631fs/19. *Middle*, the expression of Myc-tagged C terminus KvLQT1-WT, -delV595, and -P631fs/19. *Bottom*, expression of glyceraldehyde-3-phosphate dehydrogenase. Whole cell lysates were extracted from HEK293 cells 12, 24, 48, and 72 h after the transfection with equal amounts of each construct and detected with anti-c-Myc Ab or anti-glyceraldehyde-3-phosphate dehydrogenase (*GAPDH*) Ab, followed by secondary antibody. Western blot analysis showed lower expression and decreased stability of Nt-Myc-KvLQT1-delV595 and -P631fs/19 proteins as compared with Nt-Myc-KvLQT1-WT. *C*, data from representative experiments are shown. Data indicate the expression level of Myc-KvLQT1 proteins normalized by glyceraldehyde-3-phosphate dehydrogenase protein as compared with that of Nt-Myc-KvLQT1-WT protein, which was defined arbitrarily as 1.0. Densitometric data are expressed as AU and represented as means ± S.E. ($n = 4-6$ for each case). The *closed circles*, *closed triangles*, and *closed squares* represent Nt-Myc-KvLQT1-WT, -delV595, and -P631fs/19, respectively. The *open circles*, *open triangles*, and *open squares* represent Myc-tagged C terminus KvLQT1-WT, -delV595, and -P631fs/19, respectively. *, $p < 0.001$; **, $p < 0.01$; ***, $p < 0.05$ *versus* Nt-Myc-KvLQT1-WT at the same time point after the transfection.

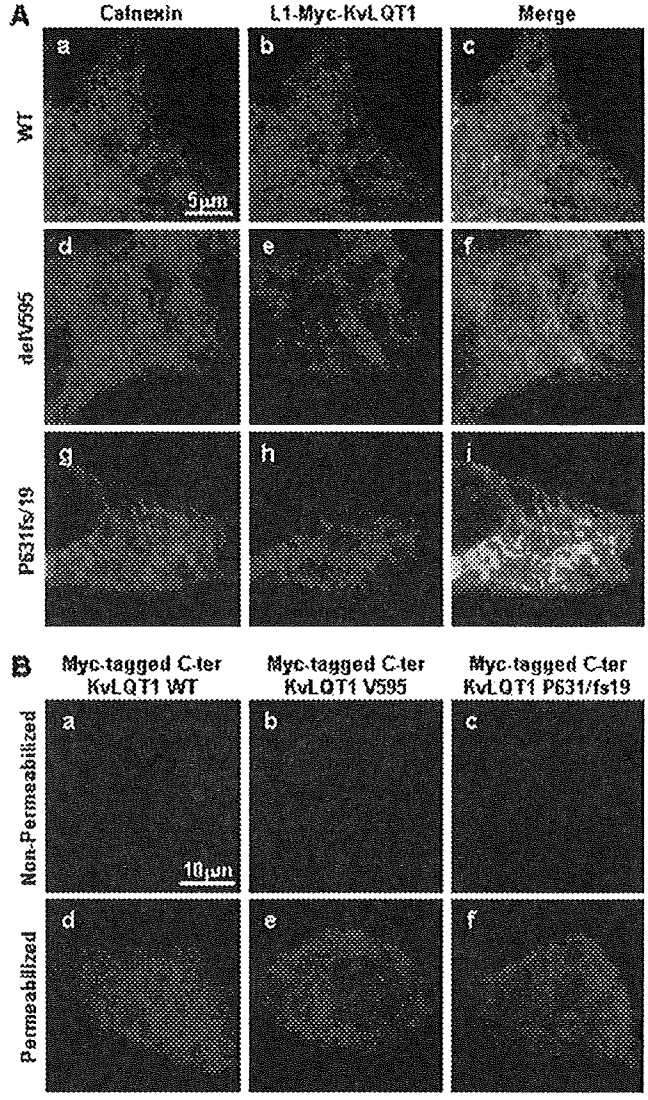

FIGURE 7. **Intracellular localization of transiently expressed Myc-tagged KvLQT1.** *A*, HEK293 cells transfected with L1-Myc-KvLQT1-WT (*a–c*), L1-Myc-KvLQT1-delV595 (*d–f*), and L1-Myc-KvLQT1-P631fs/19 (*g–i*) were fixed under the permeabilized condition and stained with anti-calnexin (*a*, *d*, and *g*) and anti-c-Myc (*b*, *e*, and *h*) Abs. Merged images are shown (*c*, *f*, and *i*). Myc-tagged mutant full-length KvLQT1 proteins, especially with the P631fs/19 mutation, showed an abnormal granular pattern, which is overlapped by the localization of calnexin. *Scale bar*, 5 μm. *B*, HEK293 cells transfected with Myc-tagged C terminus KvLQT1-WT (*a* and *d*), KvLQT1-delV595 (*b* and *e*), and KvLQT1-P631fs/19 (*c* and *f*) were fixed without (non-permeabilized conditions; *a–c*) or with (permeabilized conditions; *d–f*) 0.15% Triton X-100 and stained with anti-c-Myc Ab. C terminus KvLQT1 proteins did not express on the cell surface (*a–c*) and showed similar intracellular localizations (*d–f*). *Scale bar*, 10 μm.

gous carriers of neither delV595 nor P631fs/19 mutations showed the LQT phenotype. The most important finding in this study was that both mutations caused intracellular trafficking abnormality due to novel mechanisms, impaired complex formation (delV595), and newly generated ER retention signal (P631fs/19).

Schmitt *et al.* (11) reported that functional KvLQT1 channel complex is composed of four α-subunits, and the assembly domain in the C terminus of the α-subunit was required for the interaction of each subunit. However, all of the LQTS-associated mutations so far reported within this domain were missense mutations, N576D, T587M, G589D, A590T, R591H, R594Q, D611Y, and L619M, and the impairment of subunit binding was not demonstrated for these mutations. We also predicted the structural changes due to these mutations by using COILS and found that they would not disrupt the coiled-coil structure (data not shown), as was the case with R594Q. Because we showed that R594Q did not affect the subunit binding, it was suggested that these missense mutations might not impair the subunit assembly. On the other hand, the delV595 mutation that was predicted to disrupt the coiled-coil structure was found to impair the subunit binding in this study. In addition, we showed that the delV595 mutation reduced the intra-

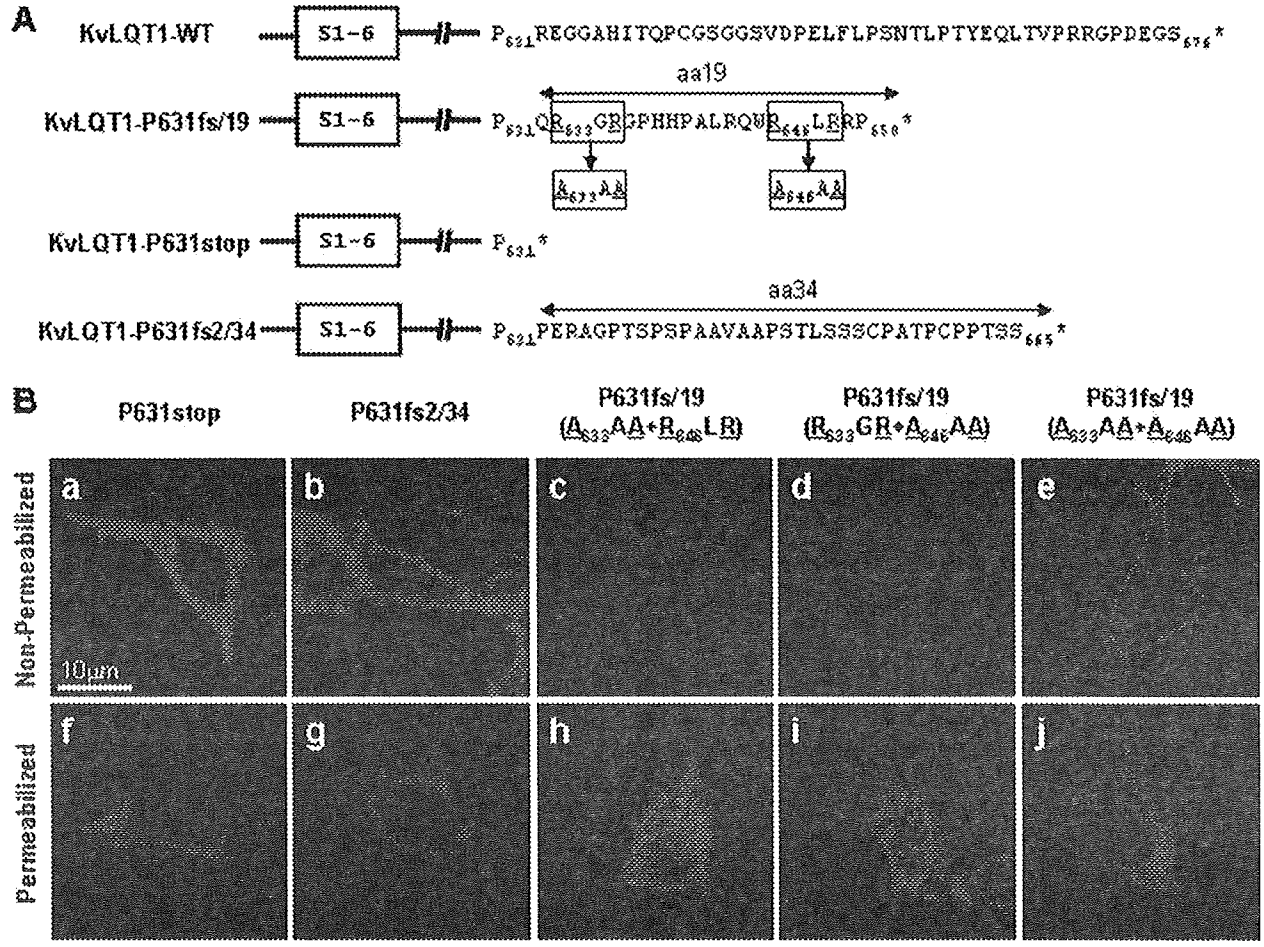

FIGURE 8. **Distribution of transiently expressed Myc-tagged KvLQT1 with or without ER retention signal.** *A*, amino acid sequences of KvLQT1 after codon 631 from WT, P631fs/19, P631stop, and P631fs2/34. Arginine residues in RGR and RLR sequences in KvLQT1-P631fs/19 mutant were substituted by alanine to investigate the role of arginines. *S1–6*, six membrane-spanning segments of KvLQT1. *, position of stop codon. *B*, HEK293 cells transfected with L1-Myc-KvLQT1-P631stop (*a* and *f*), Myc-KvLQT1-P631fs2/34 (*b* and *g*), and Myc-KvLQT1-P631fs/19 with $A^{633}AA + R^{646}LR$ (*c* and *h*), $R^{633}GR + A^{646}AA$ (*d* and *i*), or $A^{633}AA + A^{646}AA$ (*e* and *j*) were fixed without (non-permeabilized conditions) or with (permeabilized conditions) 0.15% Triton X-100 and stained with anti-c-Myc Ab. L1-Myc-KvLQT1-P631stop, -P631fs2/34, and -P631fs/19 with $A^{633}AA + A^{646}AA$ expressed well at the cell surface (*a*, *b*, and *e*) without abnormal granular pattern in the cytoplasm (*f*, *g*, and *j*), respectively. *Scale bar*, 10 μm.

cellular expression and affected the intracellular trafficking of the KvLQT1 channel, which, in turn, abolished the I_{Ks} current. These observations implied that the subunit assembly might be a prerequisite for the membrane trafficking of the KvLQT1 channel. It remains to be resolved why the impairment of subunit binding caused the intracellular trafficking abnormality, but the subunit assembly domain appeared to act as a module for proper subunit assembly and scaffolding for interaction with other proteins that are required for membrane trafficking and/or regulation of channel processing (10, 25, 29).

On the other hand, although the P631fs/19 mutation was not predicted to disrupt the coiled-coil structures, it caused the trafficking defect and complete loss of electrophysiological function of the KvLQT1 channel. Because *RGR* and *RLR* sequences similar to the ER retention signal (R*X*R motif) were found in the 19 residues generated by the frameshift, it was speculated that these two motifs caused the trafficking defect via increased retention to cytoplasmic organelle (30). Indeed, the trafficking defect of P631fs/19 was suppressed by substitutions of arginine by alanine. Reports have indicated that the R*X*R motif was used as a retention signal to ER in some channel proteins, including HERG and ATP-sensitive potassium (K_{ATP}) channels (31, 32). Although the trafficking defects were reported to cause LQTS, particularly for the HERG channel and in part for the KvLQT1 channel (17, 33, 34), the molecular mechanisms causing the defect were completely different from that of the P631fs/19 mutation found in this study. Interestingly, it was revealed that each ER retention motif was sufficient to cause the trafficking defect, because the disruption of only one motif did not suppress the retention (Fig. 8*B*).

We found that the KvLQT-P631fs/19 formed the heteromultimer with the KvLQT1-WT subunit (Fig. 4*B*), and hence it might modify the trafficking of the KvLQT1 channel containing a subunit with the P631fs/19 mutation. However, our data showed that the co-expression of KvLQT-P631fs/19 did not exert significant dominant negative effects on the current density of the KvLQT1-WT channel, indicating that the P631fs/19 mutation was a recessive mutation. In other words, the KvLQT-P631fs/19 subunit could not efficiently retain the KvLQT1-WT subunit in the cytoplasm, although these KvLQT1 subunits

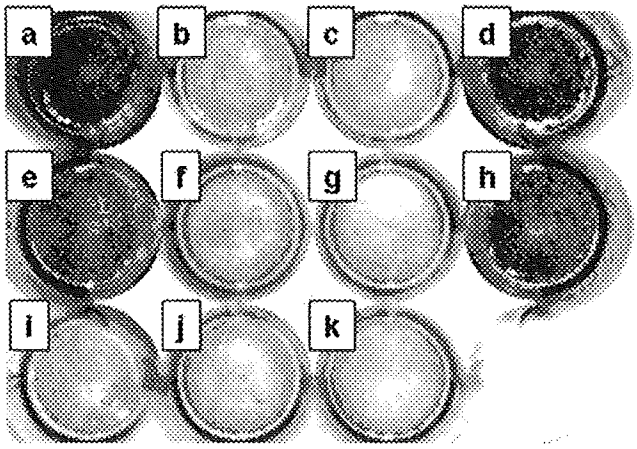

FIGURE 9. **Luminometric assay of surface expression for KvLQT1.** Cell surface expression of KvLQT1 from HEK293 transfectants (Figs. 5 and 8) was quantitatively analyzed by a luminometric assay. Representative images of the 12-well cell culture plate with confluent cells transfected with L1-Myc-KvLQT1-WT (*a*), L1-Myc-KvLQT1-delV595 (*b*), L1-Myc-KvLQT1-P631fs/19 (*c*), L1-Myc-KvLQT1-P631stop (*d*), L1-Myc-KvLQT1-P631fs2/34 (*e*), L1-Myc-KvLQT1-P631fs/19 carrying $A^{633}AA + R^{646}LR$ (*f*), L1-Myc-KvLQT1-P631fs/19 carrying $R^{633}GR + A^{646}AA$ (*g*), L1-Myc-KvLQT1-P631fs/19 carrying $A^{633}AA + A^{646}AA$ (*h*), Nt-Myc-KvLQT1-WT (*i*), Myc(−)-KvLQT1-WT (*j*), or non-transfectant (*k*) are shown.

TABLE 2

Quantitative analysis of cell surface expression of L1-Myc-KvLQT1 protein

Data are represented as means ± S.E., $n = 9$ in each assay.

Transfected construct	Chemiluminescence intensity	Relative intensity
	AU	
L1-Myc-KvLQT1-WT	592,820 ± 4,836	1.000 ± 0.008
L1-Myc-KvLQT1-delV595	102,387 ± 13,760[a]	0.173 ± 0.023[a]
L1-Myc-KvLQT1-P631fs/19	117,828 ± 11,248[a]	0.199 ± 0.019[a]
L1-Myc-KvLQT1-P631stop	560,114 ± 58,401	0.945 ± 0.099
L1-Myc-KvLQT1-P631fs2/34	537,019 ± 35,679	0.906 ± 0.060
L1-Myc-KvLQT1-P631fs/19($A^{633}AA + R^{646}LR$)	213,523 ± 36,101[a]	0.360 ± 0.061[a]
L1-Myc-KvLQT1-P631fs/19($R^{633}GR + A^{646}AA$)	121,504 ± 13,719[a]	0.205 ± 0.023[a]
L1-Myc-KvLQT1-P631fs/19($A^{633}AA + A^{646}AA$)	519,126 ± 23,794	0.876 ± 0.040
Nt-Myc-KvLQT1-WT	119,797 ± 7,856[a]	0.202 ± 0.013[a]
Myc(−)-KvLQT1-WT	57,936 ± 11,481[a]	0.098 ± 0.019[a]

[a] $p < 0.001$ *versus* chemiluminescence intensity from cells transfected with L1-Myc-KvLQT1-WT.

could form the heteromultimer. On the other hand, we found that the P631fs/19 mutation severely affected the expression and stability of full-length KvLQT1 protein in the transfectants. Therefore, the number of mutant KvLQT1 subunits was fewer than the number of normal KvLQT1 subunits in the ER, where the subunit assembly occurred. This may be the reason for the P631fs/19 mutation not exerting the dominant negative effects.

Consistent with our data, it has been reported that the individuals carrying the P631fs/19 mutation in the homozygous state but not in the heterozygous state, showed the LQTS phenotype (35). On the other hand, the P631fs/19 mutation has been reported to exhibit the Romano Ward syndrome phenotype (autosomal-dominant LQTS) (27). Why this mutation developed the LQTS phenotype in the heterozygous state in the latter report remains to be solved, but the P631fs/19 mutation might exert its abnormality in the presence of additional factors, facilitating the stability and/or heteromultimer formation in ER.

We found that the expression of full-length KvLQT1 protein was reduced by the delV595 and P631fs/19 mutations, whereas the expression of C terminus KvLQT1 was not affected by the mutations (Fig. 6). In addition, the reduced expression was more prominent with the P631fs/19 mutation than the delV595 mutation. The decreased expression of mutant KvLQT1 proteins might be due to the fact that these mutants showed trafficking abnormality and retention in the ER/Golgi apparatus, because there is a quality control of protein in ER, by which non-native and unassembled subunits of multimeric proteins are degraded by the ubiquitin-proteasome machinery (36, 37).

There are several limitations in this study. First, we used different cell lines (CHO-K1, COS-7, and HEK293) in the electrophysiological study, pull-down experiments, and cell biological experiments, respectively, leaving a possibility that we might be seeing a cell-specific effect. Second, most of the cellular experiments were done in the transiently transfected cells. Therefore, a possibility remains that the data represent the results of overexpression. Third, the direct links among the impaired subunit assembly, retention in ER, and reduced expression/stability of the delV595-KvLQT1 channel were not demonstrated at the molecular level.

In summary, we investigated functional alterations caused by *KCNQ1* mutations, delV595 and P631fs/19. These mutations were found to cause trafficking defects via different mechanisms, impaired complex formation and retention to ER, respectively. These observations provide novel insights into the molecular pathogenesis of LQTS.

Acknowledgments—We thank Dr. C. Antzelevitch and Dr. Y. Wu (Masonic Medical Research Laboratory) for helpful discussions and comments on the electrophysiological analysis. We also thank Dr. M. Yanokura, M. Emura, A. Nishimura (Tokyo Medical and Dental University), and M. Fukuoka (Hokkaido University) for technical assistance.

REFERENCES

1. Lehnart, S. E., Ackerman, M. J., Benson, D. W., Jr., Brugada, R., Clancy, C. E., Donahue, J. K., George, A. L., Jr., Grant, A. O., Groft, S. C., January, C. T., Lathrop, D. A., Lederer, W. J., Makielski, J. C., Mohler, P. J., Moss, A., Nerbonne, J. M., Olson, T. M., Przywara, D. A., Towbin, J. A., Wang, L. H., and Marks, A. R. (2007) *Circulation* **116,** 2325–2345
2. Neyroud, N., Tesson, F., Denjoy, I., Leibovici, M., Donger, C., Barhanin, J., Fauré, S., Gary, F., Coumel, P., Petit, C., Schwartz, K., and Guicheney, P. (1997) *Nat. Genet.* **15,** 186–189
3. Goldenberg, I., and Moss, A. J. (2008) *J. Am. Coll. Cardiol.* **51,** 2291–2300
4. Wang, Q., Curran, M. E., Splawski, I., Burn, T. C., Millholland, J. M., VanRaay, T. J., Shen, J., Timothy, K. W., Vincent, G. M., de Jager, T., Schwartz, P. J., Toubin, J. A., Moss, A. J., Atkinson, D. L., Landes, G. M., Connors, T. D., and Keating, M. T. (1996) *Nat. Genet.* **12,** 17–23
5. Curran, M. E., Splawski, I., Timothy, K. W., Vincent, G. M., Green, E. D., and Keating, M. T. (1995) *Cell* **80,** 795–803
6. Napolitano, C., Priori, S. G., Schwartz, P. J., Bloise, R., Ronchetti, E., Nastoli, J., Bottelli, G., Cerrone, M., and Leonardi, S. (2005) *JAMA* **294,** 2975–2980
7. Yang, W. P., Levesque, P. C., Little, W. A., Conder, M. L., Shalaby, F. Y., and Blanar, M. A. (1997) *Proc. Natl. Acad. Sci. U.S.A.* **94,** 4017–4021
8. Sanguinetti, M. C., Curran, M. E., Zou, A., Shen, J., Spector, P. S., Atkinson, D. L., and Keating, M. T. (1996) *Nature* **384,** 80–83

9. Schmitt, N., Calloe, K., Nielsen, N. H., Buschmann, M., Speckmann, E. J., Schulze-Bahr, E., and Schwarz, M. (2007) *Biochem. Biophys. Res. Commun.* **358,** 304–310
10. Chen, L., Marquardt, M. L., Tester, D. J., Sampson, K. J., Ackerman, M. J., and Kass, R. S. (2007) *Proc. Natl. Acad. Sci. U.S.A.* **104,** 20990–20995
11. Schmitt, N., Schwarz, M., Peretz, A., Abitbol, I., Attali, B., and Pongs, O. (2000) *EMBO J.* **19,** 332–340
12. Jespersen, T., Membrez, M., Nicolas, C. S., Pitard, B., Staub, O., Olesen, S. P., Baró, I., and Abriel, H. (2007) *Cardiovasc. Res.* **74,** 64–74
13. Li, X., Xu, J., and Li, M. (1997) *J. Biol. Chem.* **272,** 705–708
14. Schulteis, C. T., Nagaya, N., and Papazian, D. M. (1998) *J. Biol. Chem.* **273,** 26210–26217
15. Phartiyal, P., Jones, E. M., and Robertson, G. A. (2007) *J. Biol. Chem.* **282,** 9874–9882
16. Gong, Q., Anderson, C. L., January, C. T., and Zhou, Z. (2002) *Am. J. Physiol. Heart Circ. Physiol.* **283,** H77–H84
17. Anderson, C. L., Delisle, B. P., Anson, B. D., Kilby, J. A., Will, M. L., Tester, D. J., Gong, Q., Zhou, Z., Ackerman, M. J., and January, C. T. (2006) *Circulation* **113,** 365–373
18. Zhou, Z., Gong, Q., Epstein, M. L., and January, C. T. (1998) *J. Biol. Chem.* **273,** 21061–21066
19. Sanguinetti, M. C., Jiang, C., Curran, M. E., and Keating, M. T. (1995) *Cell* **81,** 299–307
20. Lupas, A., Van Dyke, M., and Stock, J. (1991) *Science* **252,** 1162–1164
21. Aizawa, Y., Ueda, K., Scornik, F., Cordeiro, J. M., Wu, Y., Desai, M., Guerchicoff, A., Nagata, Y., Iesaka, Y., Kimura, A., Hiraoka, M., and Antzelevitch, C. (2007) *J. Cardiovasc. Electrophysiol.* **18,** 972–977
22. Inagaki, N., Hayashi, T., Arimura, T., Koga, Y., Takahashi, M., Shibata, H., Teraoka, K., Chikamori, T., Yamashina, A., and Kimura, A. (2006) *Biochem. Biophys. Res. Commun.* **342,** 379–386
23. Arimura, T., Hayashi, T., Matsumoto, Y., Shibata, H., Hiroi, S., Nakamura, T., Inagaki, N., Hinohara, K., Takahashi, M., Manatsu, S. I., Sasaoka, T., Izumi, T., Bonne, G., Schwartz, K., and Kimura, A. (2007) *Biochem. Biophys. Res. Commun.* **357,** 162–167
24. Wu, L., Yong, S. L., Fan, C., Ni, Y., Yoo, S., Zhang, T., Zhang, X., Obejero-Paz, C. A., Rho, H. J., Ke, T., Szafranski, P., Jones, S. W., Chen, Q., and Wang, Q. K. (2008) *J. Biol. Chem.* **283,** 6968–6978
25. Kanki, H., Kupershmidt, S., Yang, T., Wells, S., and Roden, D. M. (2004) *J. Biol. Chem.* **279,** 33976–33983
26. Margeta-Mitrovic, M. (2002) *Methods* **27,** 311–317
27. Neyroud, N., Richard, P., Vignier, N., Donger, C., Denjoy, I., Demay, L., Shkolnikova, M., Pesce, R., Chevalier, P., Hainque, B., Coumel, P., Schwartz, K., and Guicheney, P. (1999) *Circ. Res.* **84,** 290–297
28. Splawski, I., Shen, J., Timothy, K. W., Lehmann, M. H., Priori, S., Robinson, J. L., Moss, A. J., Schwartz, P. J., Towbin, J. A., Vincent, G. M., and Keating, M. T. (2000) *Circulation* **102,** 1178–1185
29. Robinson, J. M., and Deutsch, C. (2005) *Neuron* **45,** 223–232
30. Michelsen, K., Yuan, H., and Schwappach, B. (2005) *EMBO Rep.* **6,** 717–722
31. Phartiyal, P., Sale, H., Jones, E. M., and Robertson, G. A. (2008) *J. Biol. Chem.* **283,** 3702–3707
32. Zerangue, N., Schwappach, B., Jan, Y. N., and Jan, L. Y. (1999) *Neuron* **22,** 537–548
33. Delisle, B. P., Anson, B. D., Rajamani, S., and January, C. T. (2004) *Circ. Res.* **94,** 1418–1428
34. Wilson, A. J., Quinn, K. V., Graves, F. M., Bitner-Glindzicz, M., and Tinker, A. (2005) *Cardiovasc. Res.* **67,** 476–486
35. Novotny, T., Kadlecova, J., Janousek, J., Gaillyova, R., Bittnerova, A., Florianova, A., Sisakova, M., Toman, O., Chroust, K., Papousek, I., and Spinar, J. (2006) *Pacing Clin. Electrophysiol.* **29,** 1013–1015
36. Nakatsukasa, K., and Brodsky, J. L. (2008) *Traffic* **9,** 861–870
37. Vembar, S. S., and Brodsky, J. L. (2008) *Nat. Rev. Mol. Cell Biol.* **9,** 944–957

Case Report

Aborted Sudden Cardiac Death Associated with Short QT Syndrome

Kaoru Okishige MD*1, Koji Sugiyama MD*1, Minetaka Maeda MD*1, Hiroshi Aoyagi MD*1, Manabu Kurabayashi MD*1, Naoto Miyagi MD*1, Daisuke Ueshima MD*1, Koji Asegawa MD*1, Tatsuhiro Takei MD*2, Toshitaka Iijin MD*1, Naomasa Makita MD*3

*1Heart Center, Yokohama-city Bay Red Cross Hospital
*2Department of Internal Cure Medicine, Nagasaki University, Graduate School of Medicine
*3Department of Physiology, Nagasaki University, Graduate School of Medicine

A 43-year-old male was transferred to our institute. His heart rhythm on admission was ventricular fibrillation (VF) which was successfully defibrillated with a direct current shock (DC). A diagnosis of short QT syndrome (SQTS) was made on the basis of an abnormally short QT interval of 280ms during the sinus rhythm. During treatment for mild total hypothermia, VF recurred repeatedly necessitating DCs. Nifekalant at a dose of 0.3 mg/kg was intravenously administered, the QT interval was prolonged from 280 to 370 ms and VF no longer recurred. Subsequently the patient underwent implantation of an implantable cardioverter defibrillator.
(J Arrhythmia 2009; 25: 214–218)

Key words: Short QT syndrome, Ventricular fibrillation, Implantable devices, Antiarrhythmic agent

Case Report

A 43-year-old male suddenly passed out while working at his desk, and bystanders who witnessed it immediately performed cardiopulmonary resuscitation on him. Despite their efforts, he did not regain consciousness, and they then called for an ambulance. The ambulance transferred him to the emergency room of our institute. His cardiac rhythm upon arrival was VF, and direct current shock (DC) was immediately delivered, resulting in the resumption of sinus rhythm (SR). Serum potassium and calcium concentrations were 3.9 and 9.2 mEq/L, respectively, and arterial blood pH was 6.94. He then underwent treatment for total mild hypothermia to improve his cerebral status which had suffered from brain damage caused by the cardiac arrest. The patient had no history of cardiovascular disease except for the paroxysmal atrial fibrillation. There was no history of sudden death in his family. He had been undergoing treatment for pure red cell aplasia for the past 10 years, and had received many blood transfusions for his anemia. During the total mild hypothermia (34 °C), he had experienced repeated VF attacks which necessitated DCs to regain SR. In order to suppress the incidence of VF, nifekalant, a pure Ikr blocker, was intravenously administered to prolong his QT interval. Continuous intravenous

Received 22 June, 2009; accepted 1 September, 2009
Address for correspondence: Kaoru Okishige MD, Heart Center, Yokohama-city Bay Red Cross Hospital, 3-12-1 Sun Tomioka Nishi-ku, Yokohama, Kanagawa 231-8682 Japan. tel: 81-45-628-5161, fax: 81-45-628-5161, E-mail: okishige@yamaguchi-u.ac.jp

nifekalant was started at a dose of 0.2 mg/kg and then increased to 0.4 mg/kg. A routine 12-lead electrocardiogram revealed SR with a significant prolongation of the QT interval from 280 to 370 ms (Bazett-corrected QT interval of 320–410 ms). The QT interval was measured from the onset of the Q wave to the terminal portion of the T wave. The configuration of the QRS complex was similar to an "Osborn wave", and may have been associated with the total hypothermia. Further, the slurring and notching of the terminal portion of the QRS complex might have been a manifestation of the transmural electrical inhomogeneity leading to the serious arrhythmias[11] (**Figure 1**) and peaked T waves that were observed as the nifekalant dose was increased to 0.4 mg/kg/hour. As the QT interval became prolonged by the intravenous nifekalant, the incidence of VF was significantly suppressed (**Figure 2**). The serum potassium concentration was maintained within normal limits and ranged from 4.1 to 5.3 μmol/l throughout his clinical course. Nifekalant was withdrawn when the QT interval significantly prolonged to a value of at least 350 ms, and frequent occurrence of VF was concomitantly and completely suppressed. The QT interval was maintained at approximately 370 ms even after the withdrawal of the nifekalant. After the total mild hypothermia, his consciousness recovered to a normal level. He underwent coronary angiography, ventriculography, and a myocardial biopsy for further examination of the etiology of his pathological status. The biopsy specimen was obtained from the right ventricular septum.

There was no evidence of abnormal coronary arteries or left ventricular function. An electrophysiological study (EPS) was also performed at the clinic to assess his VF 21 days after the cessation of the intravenous nifekalant. The effective refractory period (ERP) of the ventricles was 160 ms at a basic cycle length of 600 ms, which was measured through the electrode catheter positioned at the right ventricular apex. EPS was not performed at any other ventricular location. VF was easily and repeatedly induced by double ventricular extrastimuli (VPE) at a basic cycle length of 600 ms (**Figure 3**). EPS for the assessment of the effects of the antiarrhythmic agents was not performed. Because the ERP of his ventricles was too short, the coupling intervals of the double VPE, which were able to provoke VF, were 170 and 160 ms, respectively. He underwent implantation of an implantable cardioverter defibrillator (ICD). The diagnosis suggested by the myocardial biopsy was myocardial hemochromatosis and was characterized by deposits of hemosiderin in

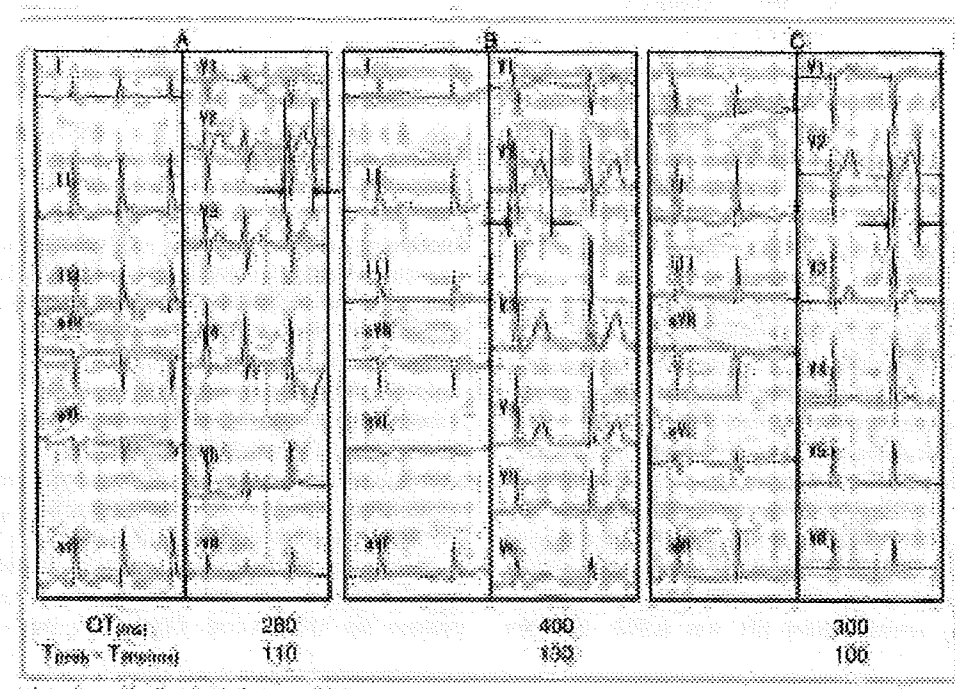

Figure 1 Twelve-lead electrocardiogram
The QT interval was prolonged from 280 ms (on admission, panel A) to 370 ms (panel B) when intravenous nifekalant was administered, and then shortened back to 300 ms (panel C) when the nifekalant was withdrawn.

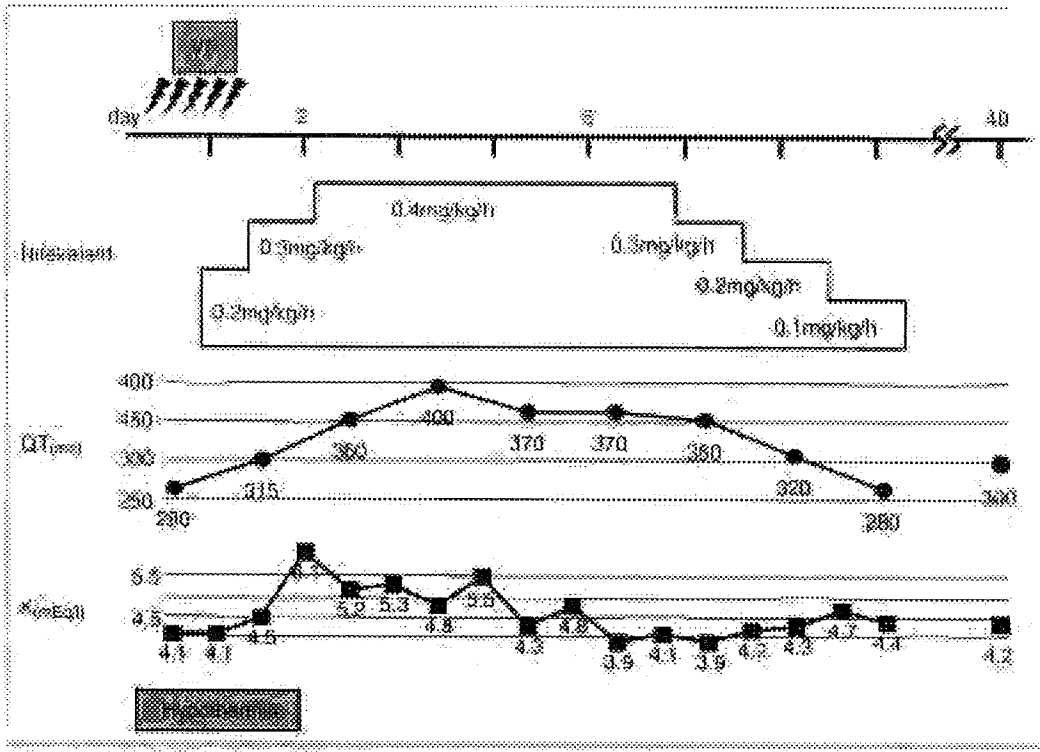

Figure 3 The clinical course in the case.
Since the QT interval was prolonged by the intravenous nifekalant, the incidence of VF significantly increased.

the myocardium. The ejection fraction of the left ventricle was approximately 57% calculated from transthoracic echocardiography. A genetic screening test was also given. The target genes were KCNH2,[3,8] KCNQ1,[3] KCNJ2,[8] as well as KCNE1 and KCNE2. However, as a result no mutations of those genes were found. Twelve-lead ECG tracings from his parents and children were examined, and no abnormal findings were recognized.

Discussion

Unlike QT prolongation, an abbreviation of the QT interval had not been considered to pose any arrhythmic risk until the publication by Gussak et al.[9] identifying that phenotype as a new clinical entity associated with an arrhythmic burden. In addition, short QT interval is not associated with any electrolyte imbalance or metabolic abnormality just as was seen in the present case. In patients with a prolonged QT interval, the Bazett correction formula is used to assess the risk of a disastrous outcome; however, Extramiana et al. demonstrated that the formula was not appropriate for making a diagnosis of SQTS because that method might induce a false negative diagnosis of SQTS.[10] Dumaine and Wolpert also reported that the rate-adaptation of the QT interval is abnormal in SQTS patients, and the QT interval may appear normal at faster heart rates when Bazett's or other corrections are applied.[8,9]

Gaita et al.[10] tested the therapeutic effects of flecainide, ibutilide, sotalol and quinidine in SQTS patients, and they found that only quinidine produced normalization of the QT interval. T wave morphology and ventricular ERP, which were described as characteristics peculiar to SQTS by Antzelevitch and Giustetto,[1,12] They further suggested that not only the blockade action of I_{Kr} but also quinidine's other properties were effective for treating SQTS. In our case, nifekalant, a pure I_{Kr} blocker, was effective for dramatically suppressing the electrical storms of VF, although it is possible that the VF in the present case might have been associated with the mild hypothermia provoking a "J wave" in the setting of the SQTS. In addition, we were unable to completely exclude the possibility of VF associated with hemochromatosis.[13-15]

When we are looking for the acute effects of a drug on VF storms in STQS, this drug might be the first option for therapy. In particular, in patients who

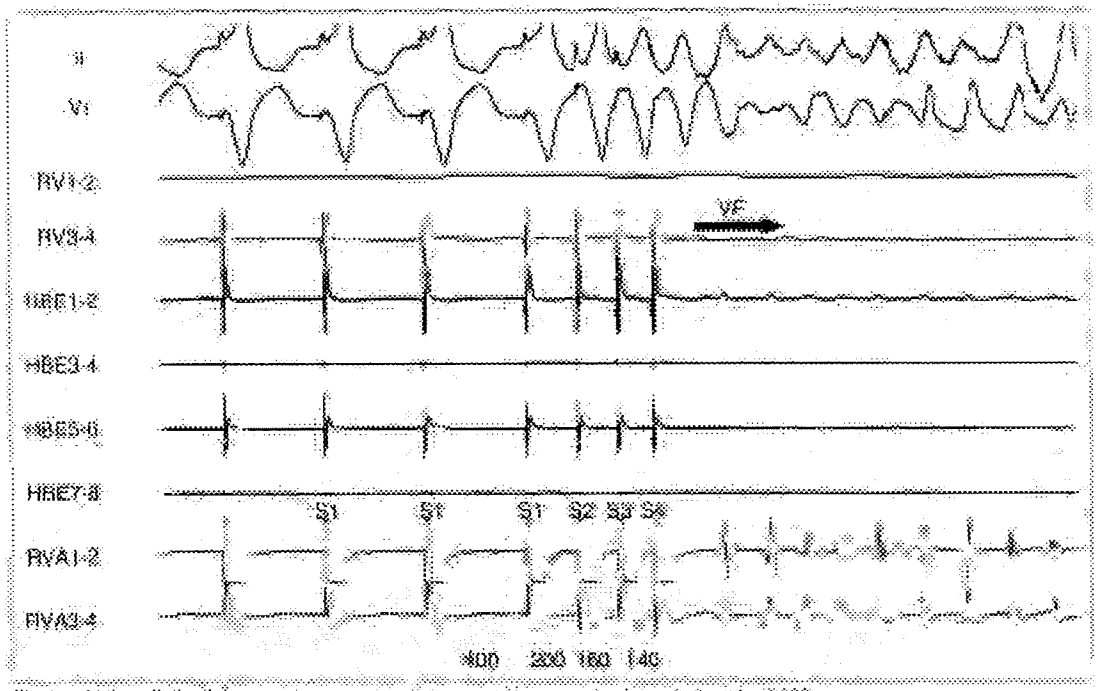

Figure 3 The ERP of the ventricles was very short at 140 ms at a basic cycle length of 600 ms. When double ventricular extrastimuli were delivered, VF was repetitively induced as shown in this figure.

are connected to artificial ventilations as in the present case, the intravenous administration of antiarrhythmic agents could be regarded as the sole therapeutic option. Antiarrhythmic Ikr blocker agents such as sotalol and quinidine could also be prescribed for chronic prophylactic treatment for VF.

The diagnosis of hemochromatosis was made according to the results of the myocardial biopsy. However, to our knowledge, there are no reports of a relationship between hemochromatosis and SQTS associated with VF.

We considered the VF in the present case to be unassociated with the electrolyte imbalance and the metabolic acidosis.

In view of the generally insufficient evidence of the protective effects of pharmacological interventions, the possibility of terminating potentially life-threatening episodes of malignant ventricular tachyarrhythmias by electrical shocks delivered from ICDs has become increasingly attractive.[15] Therefore, an appropriate risk stratification provides a rational basis for proposing an ICD implantation with a reasonable risk-benefit ratio. Although the significance of programmed pacing as another regarding the risk stratification,[15] we regarded the ease and reproducibility of VF as significant findings. Therefore we made a decision to implant an ICD in this patient. Atrial fibrillation (AF) may be the first symptom of SQTS, especially in relatively younger patients with lone AF,[16,17] and our patient also had multiple episodes of AF. He was followed up for a year, no shocks have been delivered up to the present without the use of any antiarrhythmic agents. SQTS is a rare, mechanistically heterogeneous and incompletely understood disorder. The primary treatment is an ICD implantation even though this is suboptimal. Despite agreement that effective drug therapy for SQTS is necessary, there are limited opportunities for clinical drug testing in this rare disease. Nafikalant could be regarded as the first line antiarrhythmic agent for acute dysrhythmic events in short QT syndrome.

References

1) Hassaguerre M, Derval N, Sacher F, Jesel L, Deisenhofer I, Roy L, et al: Sudden Cardiac Arrest Associated with Early Repolarization. N Engl J Med 2008; 358: 2016-2023
2) Sanguinetti MC, Jiang C, Curran ME, Keating MT: A mechanistic link between an inherited and an acquired cardiac arrhythmia: HERG encodes the IKr potassium channel. Cell 1995; 81: 299-307
3) Brugada R, Hong K, Dumaine R, Cordeiro J, Gaita F, Borggrefe M, Menendez TM, Brugada J, Pollevick GD,

Weigert C, Barashnikov E, Matsuo K, Sheng Y, Cuerchicoff A, Bianchi F, Guarino C, Schimpf R, Brugada P, Antzelevitch C: Sudden Death Associated with Short-QT Syndrome Linked to Mutation in HERG. Circulation 2004; 109: 30-35

4) Bellocq C, Van Ginneken AC, Bezzina CR, Alders M, Escande D, Mannens MM: Mutation in the KCNQ1 gene leading to the short QT interval syndrome. Circulation 2004; 109: 2394-2397

5) Priori SG, Pandit SV, Rivolta I, Berenfeld O, Ronchetti E, Dhamoon A: A novel form of short QT syndrome (SQT3) is caused by a mutation in the KCNJ2 gene. Circ Res 2005; 96: 800-807

6) Gussak I, Brugada P, Brugada J, Wright RS, Kopecky SL, Chaitman BR: Idiopathic short QT interval: a new clinical syndrome? Cardiology 2000; 94: 99-102

7) Extramiana F, Maury P, Maison-Blanche P, Dupuy A, Delay M, Leenhardt A: Electrocardiographic biomarkers of ventricular repolarisation in a single family of short QT syndrome and the role of the bazett Correction Formula. Am J Cardiol 2008; 101: 855-860

8) Dumaine R: Disopyramide: Although potentially life-threatening in the setting of long QT, could it be life-saving in short QT syndrome? J Mol and Cell Cardiol 2006; 41: 421-423

9) Wolpert C, Schimpf R, Giustetto C, Antzelevitch C, Cordeiro J, Dumaine R, Brugada R, Hong K, Bauersfeld U, Gaita F, Borggrefe M: Further insights into the effect of quinidine in short QT syndrome caused by a mutation in HERG. J Cardiovasc Electrophysiol 2005; 16: 54-58

10) Gaita F, Giustetto C, Bianchi F, Schimpf R, Haissaguerre M, Calo L, Brugada R, Antzelevitch C, Borggrefe M, Wolpert C: Short QT syndrome: Pharmacological treatment. J Am Coll Cardiol 2004; 43: 1494-1499

11) Antzelevitch C, Pollevick GD, Cordeiro JM, Casis O, Sanguinetti MC, Aizawa Y, Guerchicoff A, Pfeiffer R, Oliva A, Wollnik B, Gelber P, Bonaros EP, Burashnikov E, Wu Y, Sargent JD, Schickel S, Oberheiden R, Bhatia A, Hsu LF, Haissaguerre M, Schimpf R, Borggrefe M, Wolpert C: Loss-of-function mutation in the cardiac calcium channel underlie a new clinical entity characterized by ST segment elevation, short QT intervals, and sudden cardiac death. Circulation 2007; 115: 442-449

12) Giustetto C, Monte FD, Wolpert C, Borggrefe M, Schimpf R, Sbragia P, Leone G, Maury P, Anttonen O, Haissaguerre M, Gaita F: Short QT syndrome: clinical findings and diagnostic-therapeutic implications. Eur Heart J 2006; 27: 2440-2447

13) Yalcinkaya S, Kumbasar SD, Semiz E, Tosun Z, Pekdemir N: Sustained ventricular tachycardia in cardiac hemochromatosis treated with amiodarone. J Electrocardiol 1997; 30: 147-149

14) Strobel JS, Fuisz AR, Epstein AE, Plumb VJ: Syncope and inducible ventricular fibrillation in a woman with hemochromatosis. J Interv Card Electrophysiol 1999; 3: 225-229

15) Bonanni G, Bifil M, Valzania C, Bronzetti G, Martignani C: Short QT syndrome and arrhythmogenic cardiac diseases in the young: the challenge of implantable cardioverter-defibrillator therapy for children. Eur Heart J 2006; 27: 2383-2384

16) Lu LX, Zhou W, Zhang X, Cao Q, Yu K, Zhu C: Short QT syndrome: A case report and review of literature. Resuscitation 2006; 71: 115-121

17) Schimpf R, Wolpert C, Gaita F, Giustetto C, Borggrefe M: Short QT syndrome. Cardiovasc Res 2005; 67: 357-366

Journal of the American College of Cardiology
© 2009 by the American College of Cardiology Foundation
Published by Elsevier Inc.

Vol. 54, No. 22, 2009
ISSN 0735-1097/09/$36.00
doi:10.1016/j.jacc.2009.08.028

QUARTERLY FOCUS ISSUE: HEART RHYTHM DISORDERS

Genotype-Phenotype Aspects of Type 2 Long QT Syndrome

Wataru Shimizu, MD, PHD,* Arthur J. Moss, MD,‡ Arthur A. M. Wilde, MD, PHD,‖ Jeffrey A. Towbin, MD,# Michael J. Ackerman, MD, PHD,** Craig T. January, MD, PHD,†† David J. Tester, BS,** Wojciech Zareba, MD, PHD,‡ Jennifer L. Robinson, MS,‡ Ming Qi, PHD,§ G. Michael Vincent, MD,‡‡ Elizabeth S. Kaufman, MD,§§ Nynke Hofman, MSc,¶ Takashi Noda, MD, PHD,* Shiro Kamakura, MD, PHD,* Yoshihiro Miyamoto, MD, PHD,† Samit Shah, BA,‡ Vinit Amin, MA,‡ Ilan Goldenberg, MD,‡ Mark L. Andrews, BBA,‡ Scott McNitt, MS‡

Osaka, Japan; Rochester, New York; Amsterdam, the Netherlands; Houston, Texas; Rochester, Minnesota; Madison, Wisconsin; Salt Lake City, Utah; and Cleveland, Ohio

Objectives The purpose of this study was to investigate the effect of location, coding type, and topology of *KCNH2(hERG)* mutations on clinical phenotype in type 2 long QT syndrome (LQTS).

Background Previous studies were limited by population size in their ability to examine phenotypic effect of location, type, and topology.

Methods Study subjects included 858 type 2 LQTS patients with 162 different *KCNH2* mutations in 213 proband-identified families. The Cox proportional-hazards survivorship model was used to evaluate independent contributions of clinical and genetic factors to the first cardiac events.

Results For patients with missense mutations, the transmembrane pore (S5-loop-S6) and N-terminus regions were a significantly greater risk than the C-terminus region (hazard ratio [HR]: 2.87 and 1.86, respectively), but the transmembrane nonpore (S1–S4) region was not (HR: 1.19). Additionally, the transmembrane pore region was significantly riskier than the N-terminus or transmembrane nonpore regions (HR: 1.54 and 2.42, respectively). However, for nonmissense mutations, these other regions were no longer riskier than the C-terminus (HR: 1.13, 0.77, and 0.46, respectively). Likewise, subjects with nonmissense mutations were at significantly higher risk than were subjects with missense mutations in the C-terminus region (HR: 2.00), but that was not the case in other regions. This mutation location–type interaction was significant ($p = 0.008$). A significantly higher risk was found in subjects with mutations located in α-helical domains than in subjects with mutations in β-sheet domains or other locations (HR: 1.74 and 1.33, respectively). Time-dependent β-blocker use was associated with a significant 63% reduction in the risk of first cardiac events ($p < 0.001$).

Conclusions The *KCNH2* missense mutations located in the transmembrane S5-loop-S6 region are associated with the greatest risk. (J Am Coll Cardiol 2009;54:2052–62) © 2009 by the American College of Cardiology Foundation

From the *Division of Cardiology, Department of Internal Medicine, and †Laboratory of Molecular Genetics, National Cardiovascular Center, Suita, Osaka, Japan; ‡Cardiology Division, Department of Medicine, and the §Department of Pathology, University of Rochester School of Medicine and Dentistry, Rochester, New York; Departments of ‖Cardiology and ¶Clinical Genetics, Academic Medical Center, Amsterdam, the Netherlands; #Department of Pediatrics, Baylor College of Medicine, Texas Children's Hospital, Houston, Texas; **Departments of Medicine, Pediatrics, and Molecular Pharmacology, Mayo Clinic College of Medicine, Rochester, Minnesota; ††Departments of Medicine and Physiology, University of Wisconsin-Madison, Madison, Wisconsin; ‡‡University of Utah, School of Medicine, Salt Lake City, Utah; and the §§Heart and Vascular Research Center, MetroHealth Campus of Case Western Reserve University, Cleveland, Ohio. Dr. Ackerman has a consulting relationship and license agreement/royalty arrangement with PGxHealth (FAMILION). This work was supported in part by a Health Sciences Research Grant (H18-Research on Human Genome-002) and a Research Grant for the Cardiovascular Diseases (21C-8) from the Ministry of Health, Labour and Welfare, Japan (to Dr. Shimizu); research grants HL-33843 and HL-51618 (to Dr. Moss) and HL-60723 (to Dr. January) from the National Institutes of Health, Bethesda, Maryland; and grant 2000.059 from the Nederlandse Hartstichting, Amsterdam, the Netherlands (to Dr. Wilde). Dr. Ackerman has received support from Medtronic, PGxHealth, and Pfizer. Dr. January has received support from Cellular Dynamics International. Dr. Tester receives modest royalties from PGxHealth. Dr. Kaufman receives research support from CardioDx and St. Jude Medical. Drs. Shimizu, Moss, Wilde, Towbin, Ackerman, and January contributed equally to the original concept of this investigation.

Manuscript received May 31, 2009; revised manuscript received August 14, 2009, accepted August 24, 2009.

Long QT syndrome (LQTS) is a congenital disorder caused by mutations of several cardiac ion channel genes and is diagnosed clinically by a prolonged QT interval on the electrocardiogram (ECG) and variable clinical outcomes including arrhythmia-related syncope and sudden death (1,2). Mutations involving the *KCNH2* gene (*hERG* [human ether-a-go-go-related gene]), which codes for the pore-forming α-subunit of a cardiac K^+ channel, have been linked to the type 2 LQTS, the second most common variant of LQTS (3). The *KCNH2* mutations lead to a reduction in the rapid component of the delayed rectifier repolarizing current (I_{Kr}), which contributes to lengthening of the QT interval (4). The *KCNH2* subunits oligomerize to form a tetramer that inserts into the cell membrane to form the functional K^+ channel. Each subunit comprises 6 α-helical transmembrane segments (S1 to S6), where the K^+-selective pore is found between S5 and S6. The transmembrane segments are flanked by amino (N)- and carboxyl (C)-terminus regions (5–8). In a previous study of patients with type 2 LQTS, mutations in the pore region were associated with an increased risk for arrhythmia-related cardiac events when compared with patients with nonpore mutations (9). However, this study was limited by population size in its ability to examine the phenotypic effect of mutations within distinct domains of the nonpore region.

See page 2063

There are several coding types of mutations in genes that form the functional K^+ channel: missense, nonsense, splice site, in-frame deletion, and frameshift mutations (10). Missense mutations are point mutations that result in a single amino acid change within the protein; nonsense mutations generate a stop codon and can truncate the protein. Insertion and deletion mutations cause in-frame or frameshift mutations, the latter of which change the grouping of nucleotide bases into codons. Splice site mutations may alter splicing of messenger ribonucleic acid. In our recent cohort of type 1 LQTS (11), a missense mutation accounted for 81% of all the mutations, and the type of mutation (missense vs. nonmissense) was not an independent risk factor. On the other hand, nonmissense mutations such as frameshift and nonsense mutations have been reported to be more frequently identified in the type 2 LQTS patients (11,12).

Moreover, topology of mutations (α-helical domain, β-sheet domain, and other uncategorized location) has been recently reported to relate to the function of mutated channel in the type 2 LQTS patients (8).

We hypothesized that the distinct location, coding type, and topology of the channel mutation would have important influence on the phenotypic manifestations and clinical course of patients with type 2 LQTS. To test this hypothesis, we investigated the clinical aspects of 858 subjects having a spectrum of *KCNH2* mutations categorized by the distinct location, coding type, and topology of the channel mutations.

Abbreviations and Acronyms

ECG = electrocardiogram

I_{Kr} = rapid component of the delayed rectifier repolarizing current

LQTS = long QT syndrome

NMD = nonsense-mediated decay

QTc = corrected QT

Methods

Study population. The study population of 858 subjects was derived from 213 proband-identified families with genetically confirmed *KCNH2* mutations. The proband in each family had corrected QT (QTc) prolongation not due to a known cause. The subjects were drawn from the U.S. portion of the International LQTS (Rochester) Registry (n = 456), the Netherlands' (Amsterdam) LQTS Registry (n = 214), the Japanese (National Cardiovascular Center) LQTS Registry (n = 95), and the Mayo Clinic LQTS Registry (n = 93). All subjects or their guardians provided informed consent for the genetic and clinical studies. Not included in the study population were 58 subjects with evidence of 2 or more LQTS mutations and an additional 18 who had polymorphisms (p.R176W or p.R1047L) that the authors felt might reduce I_{Kr} current. A total of 201 of the 456 patients enrolled from the U.S. portion of the International LQTS Registry and 61 of the 95 patients from the Japanese LQTS Registry were reported in our prior reports (9,12).

Phenotype characterization. Routine clinical and electrocardiographic parameters were acquired at the time of enrollment in each of the registries. Follow-up was censored at age 41 years to minimize the influence of coronary disease on cardiac events. Measured parameters on the first recorded ECG included QT and R-R intervals in milliseconds, with QT corrected for heart rate by Bazett's formula. The QTc interval was expressed in its continuous form and categorized into 4 levels: <460, 460 to 499, 500 to 530, and >530 ms. The QTc interval was categorized into 3 levels: <500, 500 to 530, and >530 ms for the end point of lethal cardiac events (aborted cardiac arrest or LQTS-related sudden cardiac death), because there were few lethal cardiac events in the lowest QTc group (<460 ms). Clinical data were collected on prospectively designed forms with information on demographic characteristics, personal and family medical history, electrocardiographic findings, therapy, and end points during long-term follow-up. Data common to all 4 LQTS registries involving genetically identified patients with type 2 LQTS genotype were electronically merged into a common database for this study.

Genotype characterization. The *KCNH2* mutations were identified using standard genetic tests performed in molecular-genetic laboratories in the participating academic centers. From the Rochester registry, 60 subjects died of sudden cardiac death at a young age and were not genotyped. These 60 subjects were assumed to have the same

KCNH2 mutation as other affected close members of their respective family.

Genetic alterations of the amino acid sequence were characterized by location in the channel protein, by the type of mutation (missense, splice site, in-frame insertions/deletions, nonsense [stop codon], and frameshift), and by the topology of mutation (α-helical domain, β-sheet domain, and other uncategorized location) (Fig. 1). The transmembrane region of the *KCNH2* encoded channel was defined as the coding sequence involving amino acid residues from 398 through 657 (S5-loop-S6 region: 552 to 657), with the N-terminus region defined before residue 398, and the C-terminus region after residue 657 (Fig. 1) (13,14).

We evaluated the risk associated with 4 main prespecified regions: 1) N-terminus; 2) transmembrane "nonpore" region (S1–S4); 3) transmembrane "pore" region (S5-loop-S6); and 4) C-terminus. We also evaluated the risk associated with distinct types of mutation and topology of mutation.

Statistical analysis. Differences in the univariate characteristics by specific groupings were evaluated by standard statistical methods. The primary end point was time to syncope, aborted cardiac arrest, or sudden death, whichever occurred first. The cumulative probability of a first cardiac event was assessed by the Kaplan-Meier method, with significance testing by the log-rank statistic. The Cox proportional-hazards survivorship model was used to evaluate the independent contribution of clinical and genetic factors to the first occurrence of time-dependent cardiac events from birth through age 40 years (15). The Cox regression models, stratified by decade of birth year and allowing for time-dependent covariates, were fit to estimate the adjusted hazard ratio (HR) of each factor as a predictor of first cardiac events. We observed that sex was not proportional as a function of age, with crossover in risk at age 13 on univariate Kaplan-Meier analysis. To fulfill the assumption of proportional hazards for sex over the entire age range, a time-dependent covariate for sex (via an interaction with time) was incorporated, allowing for different hazard ratios by sex before and after age 13 years.

Since almost all subjects were first- and second-degree relatives of probands, the effect of potential lack of independence between subjects was evaluated by refitting the Cox model using the robust sandwich estimator for family membership (16). All significant predictors of risk maintained significance using this robust measure of variance.

Patients who did not have an ECG for QTc measurement were identified in the Cox models as "QTc missing."

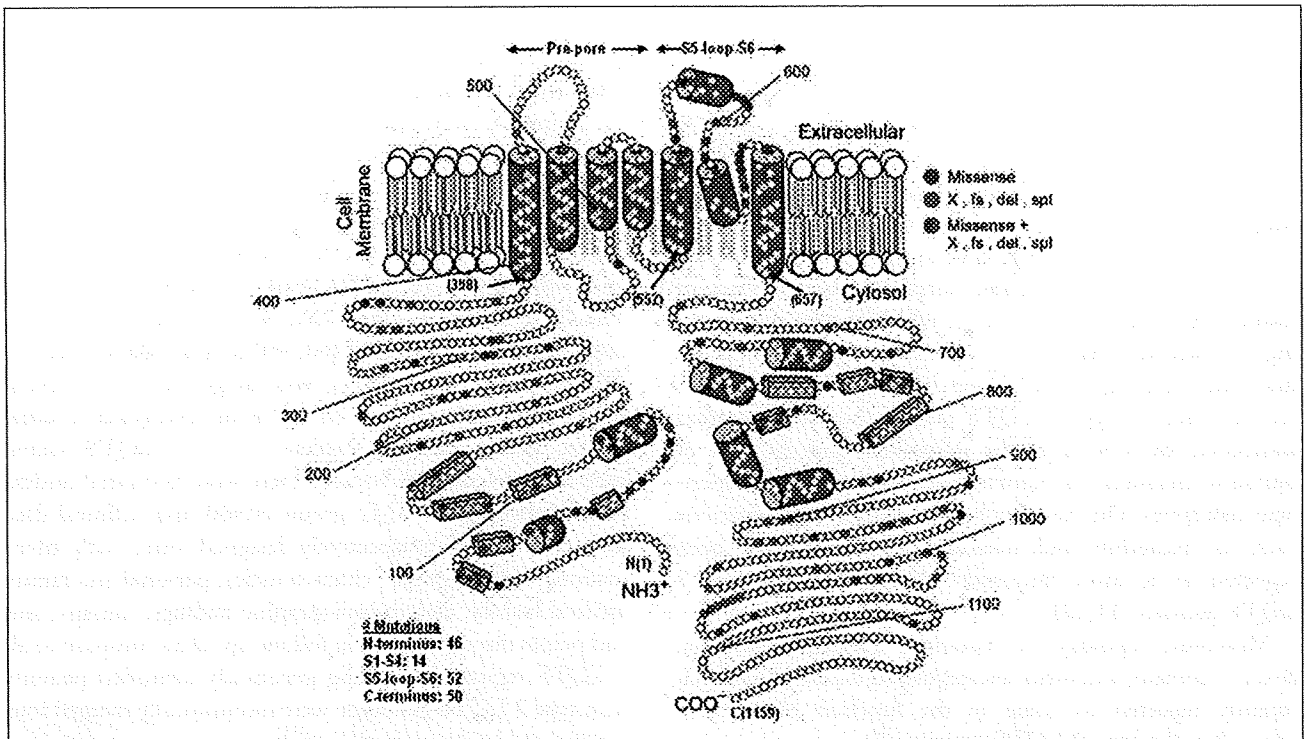

Figure 1 **Location of Different Mutations in KCNH2 Potassium Channel**

Diagramatic location of 162 different mutations in the KCNH2 potassium channel involving 858 subjects. The α subunit involves the N-terminus ($NH3^+$), 6 membrane-spanning segments, and the C-terminus portion (COO^-). The **numbers in parentheses** refer to the position of the amino acid beginning at the N-term position (1), the beginning of the transmembrane nonpore S1 to S4 sequence (398), the beginning of the transmembrane S5-loop-S6 sequence (552), the end of the transmembrane S6 sequence (657), and at the C-term end position (1,159). The **open circles** represent individual amino acids, the **red circles** indicate the missense mutations, and the **blue circles** indicate nonmissense mutations. The **cylinders** represent putative α-helical segments, and the **bars** represent putative β-sheets.

Pre-specified covariate interactions between mutation location, type, and α-helical domains were evaluated. Only the mutation location–missense interaction was significant. To test the impact of the interaction between the 4 different mutation locations and missense mutation type, 3 interaction terms were added to the Cox proportional hazards regression model. A 3 degree of freedom likelihood-ratio test was performed to determine their statistical significance. The influence of time-dependent β-blocker therapy (the age at which β-blocker therapy was initiated) on outcome was determined by adding this variable to the final Cox model containing the various covariates.

Results

Total study population. The continuum of *KCNH2* mutations and their respective number of subjects by location, type, and topology of mutation and contributing registry are presented in the Online Table, and the location, type, and topology of the mutations are diagrammatically presented in Figure 1. A total of 162 different *KCNH2* mutations were identified in 858 subjects. The mutations were predominantly found in 3 regions: the N-terminus (28.4%, n = 46), the C-terminus (30.9%, n = 50), and the transmembrane domain (40.7%, n = 66). Of the 66 mutations within the transmembrane domain, 78.8% (n = 52) were located within the S5-loop-S6 region. Missense (single amino acid substitutions) accounted for 61.7% (n = 100) of all the mutations, splice site for 1.9% (n = 3), in-frame insertions/deletions for 0.6% (n = 1), nonsense for 10.5% (n = 17), and frameshift for 25.3% (n = 41). Sixty-six mutations (40.7%) were located in the α-helical domain, 17 (10.5%) in the β-sheet domain, and 79 (48.8%) in other uncategorized locations.

The phenotypic characteristics of patients enrolled in each of the 4 registries and by location, type, and topology of mutation are presented in Table 1. The age was younger in the Mayo Clinic registry than in the other 3 registries. The QTc interval was longer and the cardiac events were more frequent in the U.S. and Japanese registries than in the other 2 registries. A pacemaker was more frequently implanted in the U.S. registry, and a defibrillator in the Mayo Clinic registry. LQTS-related death was more frequent in the U.S. registry than in the other 3 registries; that seems mainly because the U.S. registry included the largest proportion of patients missing ECG data and was the longest-standing registry, in which 44 of the 92 deaths occurred before 1980. It is not surprising that the death rate in subjects missing ECG data (i.e., QTc) was very high.

Location, type, and topology of mutation on clinical outcome. As to the location of mutation, the QTc interval was longer and cardiac events were more frequent in patients with mutations in the transmembrane pore locations (S5-loop-S6) than in patients with mutations in transmembrane nonpore (S1 to S4), N-terminus, or C-terminus locations. As to the type of mutation, the QTc interval was longer in patients with missense mutations than in patients with either frameshift/nonsense or other mutations. Sudden death was also more frequent among patients with missense mutations. As to the topology of mutation, the QTc interval was longer and cardiac events were more frequent among patients with mutations located in the α-helical domain than among patients with mutations in either the β-sheet domain or other uncategorized location.

The cumulative probabilities of first cardiac event by type, location, and topology of mutation are presented in Figures 2A, 2B, and 2C, respectively. No significant difference in event rates was observed among types of mutation (p = 0.68) (Fig. 2A), although missense mutations were more associated with longer QTc interval and increased risk for sudden death compared with other types of mutations. Conversely, significantly higher event rates were found among subjects with transmembrane pore mutations than among subjects with mutations in transmembrane nonpore, N-terminus, or C-terminus regions, with a gradual increase in event rates occurring during ages 5 to 40 years (Fig. 2B). Significantly higher event rates were also observed among subjects with mutations located in the α-helical domains than among subjects with mutations in either the β-sheet domains or other locations (Fig. 2C).

The findings from the Cox regression analysis by location and by topology of *KCNH2* mutations for first cardiac events and those for aborted cardiac arrest or LQTS-related sudden cardiac death are presented in Table 2. The clinical risk factors associated with first cardiac events involved males before age 13 years (HR: 1.54 vs. females), females after age 13 years (HR: 3.29 vs. males), and longer QTc intervals (HR: 3.33, QTc >530 ms [n = 112] vs. QTc <460 ms [n = 239]; HR: 2.09, QTc 500 to 530 ms [n = 146] vs. QTc <460 ms; HR: 1.56, QTc 460 to 499 ms [n = 251] vs. QTc <460 ms). Mutations located in the transmembrane pore region made significant and independent contributions to the risk model, with C-terminus region as reference (HR: 1.56). Mutations located in the α-helical domains made significant contributions to the risk model with the β-sheet domains as reference (HR: 1.74). A mutation in the α-helical domain located in the transmembrane pore region would have a risk equal to the multiplicative product of the 2 hazard ratios, namely, 1.56 × 1.74 = 2.71. On the other hand, a mutation in the α-helical domain located in the nonpore transmembrane S1 to S4 region would have a risk of 0.61 × 1.74 = 1.06, and this value was very similar to 1. Time-dependent β-blocker use was associated with a significant 63% reduction in the risk of first cardiac events (p < 0.001). The clinical risk factors associated with lethal cardiac events showed similar tendency to those with cardiac events, and involved females after age 13 years (HR: 2.38 vs. males) and longer QTc intervals (HR: 4.97, QTc >530 ms vs. QTc <500 ms; HR: 2.57, QTc 500 to 530 ms vs. QTc <500

Table 1 Phenotypic Characteristics by Source of Subjects, Location of Mutation, Type of Mutation, and Topology of Mutation

Characteristics	Source of Subjects				Location of Mutation				Type of Mutation			Topology of Mutation		
	Rochester	the Netherlands	Japan	Mayo	Transmembrane (S1–S4)	Transmembrane (S5-Loop-S6)	N-Terminus	C-Terminus	Missense	Frameshift/ Nonsense	Others	α-Helices	β-Sheet	Neither
Unique mutations					14	52	46	50	100	58	4	66	17	79
Patients	456	214	95	93	44	259	243	312	555	261	42	319	141	398
Female	57	59	66	57	57	59	56	60	60	56	55	57	55	61
ECG at enrollment														
Age*†‡, yrs	25 ± 20	33 ± 21	30 ± 18	22 ± 16	28 ± 16	24 ± 19	32 ± 21	26 ± 19	28 ± 20	27 ± 19	26 ± 22	25 ± 19	31 ± 22	28 ± 19
QTc*†‡§, s	0.49 ± 0.06	0.47 ± 0.05	0.49 ± 0.05	0.47 ± 0.05	0.48 ± 0.05	0.50 ± 0.06	0.47 ± 0.06	0.48 ± 0.05	0.49 ± 0.06	0.47 ± 0.05	0.47 ± 0.06	0.49 ± 0.05	0.48 ± 0.05	0.48 ± 0.06
QTp*†, s	0.34 ± 0.07	0.33 ± 0.05	0.38 ± 0.06	0.34 ± 0.06	0.37 ± 0.07	0.36 ± 0.07	0.34 ± 0.06	0.34 ± 0.07	0.35 ± 0.07	0.34 ± 0.06	0.34 ± 0.08	0.35 ± 0.07	0.33 ± 0.07	0.34 ± 0.06
Therapy														
β-blockers	51	45	45	60	48	53	45	51	49	51	50	51	48	49
Pacemaker*	6.8	0.5	1.1	0	2.3	6.6	2.5	2.9	4.5	2.7	2.4	5.6	2.8	2.8
Sympathectomy	2	0.9	0	1.1	2.3	1.5	0	2.2	1.6	0.8	2.4	1.6	2.8	0.8
Defibrillator*	14	4.7	6.3	25	18	14	8.2	12	11	13	17	12	9.9	13
First cardiac event*†‡‖	50	34	52	31	34	58	40	38	45	44	29	54	30	41
Syncope*†‡	42	31	52	28	32	49	36	34	39	39	29	45	26	38
Aborted cardiac arrest	0.7	1.9	0	3.2	2.3	1.2	1.2	1	1.3	1.1	0	1.6	0.7	1
Death*†‡	7.7	0.5	0	0	0	7.7	2.9	2.9	5.0	3.1	0	7.2	2.8	2.3
Ever cardiac event														
Syncope*†‡	42	31	55	28	32	49	36	34	39	39	29	45	26	38
Aborted cardiac arrest*	4.6	7.5	16	7.5	11	6.9	6.2	6.7	6.1	8.4	7.1	7.8	4.3	7
Death*†‡§	18	3.3	0	2.2	4.5	17	11	6.7	14	5.7	7.1	16	8.5	7.8

Values are n, %, or mean ± SD. Percentages >10 are rounded to a whole number. The 858 subjects in this table include 60 subjects from the Rochester-based registry who died suddenly at a young age, were from families with known *KCNH2* mutation, and were assumed to have the family mutation. *$p < 0.01$ for the comparison of characteristics among the 4 sources of subjects. †$p < 0.01$ for the comparison of characteristics among the 4 locations of the mutations. ‡$p < 0.01$ for the comparison of characteristics among the 3 major topologies of mutations. §$p < 0.01$ for the comparison of characteristics among the 3 major types of mutations. ‖First cardiac event was syncope, aborted cardiac arrest, or sudden death, whichever occurred first.

ECG = electrocardiogram; QTc = corrected QT; QTp = QT peak interval.

JACC Vol. 54, No. 22, 2009
November 24, 2009:2052–62

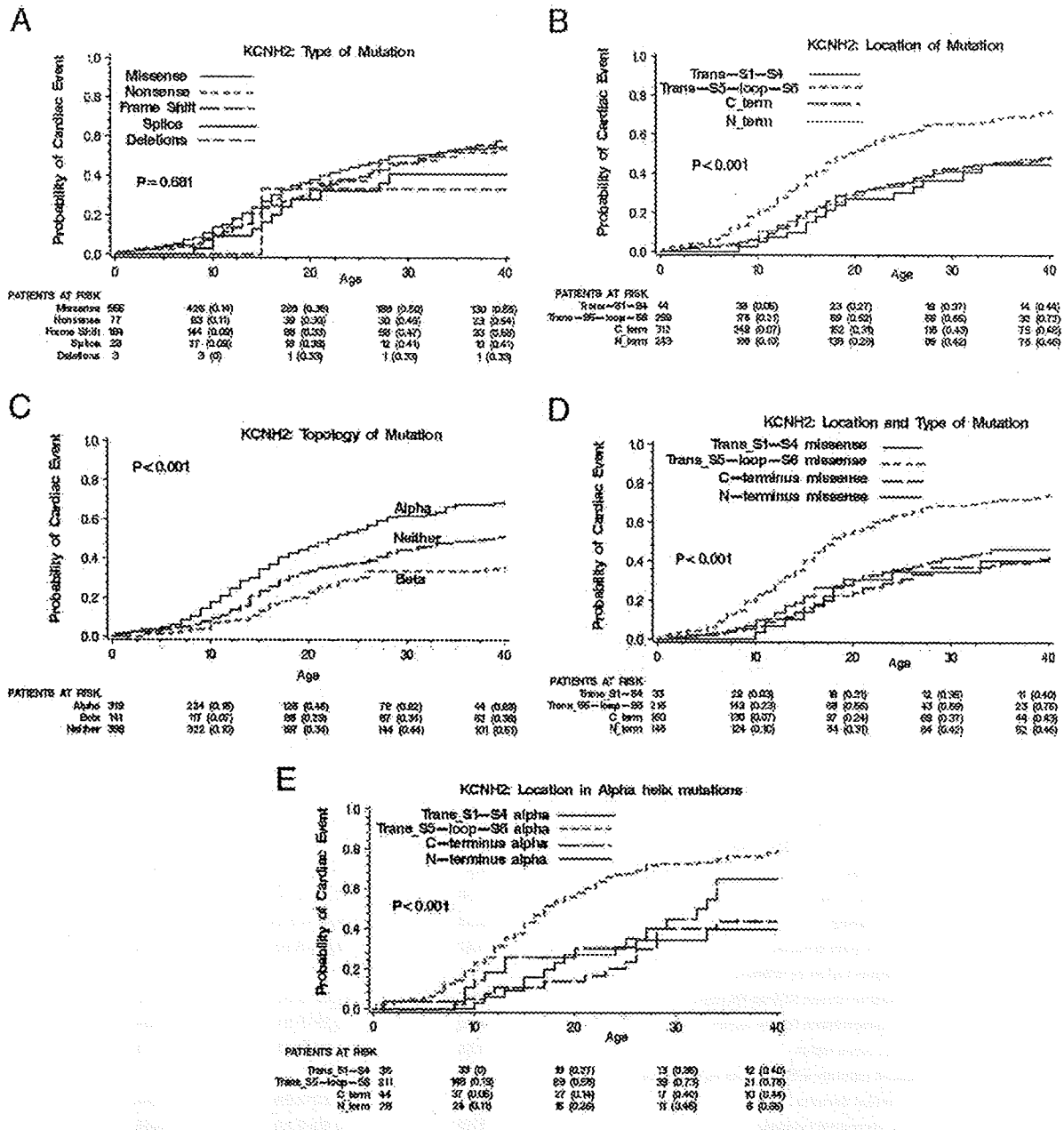

Figure 2 Kaplan-Meier Estimates of Cumulative Probability of First Cardiac Event

Kaplan-Meier estimate of the cumulative probability of a first cardiac event by **(A)** type, **(B)** location, and **(C)** topology of the mutation for all 858 subjects with genetically confirmed *KCNH2* mutations. Kaplan-Meier estimate of the cumulative probability of a first cardiac event for **(D)** missense mutations within different locations and for **(E)** mutations located in the α-helical domains within different locations. The **numbers in parentheses** reflect the cumulative event rate at that point in time.

ms). History of prior syncope was a significant risk for lethal cardiac events (HR: 3.42). Time-dependent β-blocker use showed a reduction in the risk of lethal cardiac events by 26%, but this did not reach statistical significance.

Combination of location and type of mutation on clinical outcome. The inter-relation between location, type, and topology of mutation is presented in Table 3. Among 52 mutations within the transmembrane pore region, 46 mutations (88.5%) were missense mutations, and only 6 mutations (11.5%) were frameshift/nonsense mutations. Conversely, frameshift/nonsense mutations were more frequently located in the C-terminus region (31 of 50 mutations, 62.0%); 17 mutations (34.0%) were missense mutation, and the remaining 2 mutations (4.0%) were from any other type (splice mutation). Because transmembrane pore mutations are more risky than

JACC Vol. 54, No. 22, 2009
November 24, 2009:2052–62

Table 2 Cox Regression With Multiple Predictor Variables Including Location of Mutations for First Cardiac Event and Aborted Cardiac Arrest/Long QT Syndrome Death

Variable	Hazard Ratio	95% Confidence Interval	p Value
First cardiac event			
Enrolling sites with the Netherlands as reference			
Rochester	1.38	1.03–1.85	0.030
Japan	1.10	0.74–1.63	0.644
Mayo	0.94	0.60–1.47	0.786
Sex/age			
Males/females age <13 yrs	1.54	1.08–2.20	0.018
Females/males age 13 to 40 yrs	3.29	2.36–4.60	<0.001
QTc categories with QTc <460 ms as reference, ms			
QTc >530	3.33	2.30–4.83	<0.001
QTc 500 to 530	2.09	1.45–3.02	<0.001
QTc 460 to 499	1.56	1.11–2.21	0.011
QTc missing*	3.33	2.25–4.92	<0.001
C-terminus region as reference			
Transmembrane S5-loop-S6 region	1.56	1.14–2.14	0.006
Transmembrane S1–S4 region	0.61	0.34–1.09	0.095
N-terminus region	1.22	0.92–1.62	0.173
Subunit topology with β-sheets as reference			
α-helical domains	1.74	1.15–2.63	0.009
Uncategorized locations	1.33	0.93–1.90	0.115
Time-dependent β-blocker use	0.37	0.22–0.63	<0.001
Aborted cardiac arrest/long QT syndrome death			
Enrolling sites with the Netherlands as reference			
Rochester	1.38	0.79–2.41	0.257
Japan	1.87	0.89–3.94	0.099
Mayo	1.37	0.53–3.52	0.520
Sex/age			
Males/females age <13 yrs	1.55	0.52–4.64	0.433
Females/males age 13 to 40 yrs	2.38	1.50–3.79	<0.001
QTc categories with QTc <500 ms as reference, ms			
QTc >530	4.97	2.72–9.07	<0.001
QTc 500–530	2.57	1.39–4.76	0.003
QTc missing*	25.58	14.46–45.26	<0.001
History of prior syncope	3.42	2.25–5.20	<0.001
C-terminus region as reference			
Transmembrane S5-loop-S6 region	1.00	0.56–1.80	0.993
Transmembrane S1–S4 region	1.00	0.39–2.61	0.994
N-terminus region	1.33	0.80–2.22	0.271
Subunit topology with β-sheets as reference			
α-helical domains	1.47	0.72–2.98	0.269
Uncategorized locations	1.12	0.60–2.10	0.658
Time-dependent β-blocker use	0.74	0.42–1.31	0.300

The Cox analysis involved 858 subjects with 259 transmembrane S5-loop-S6, 44 transmembrane S1 to S4, 243 N-terminus, and 312 C-terminus mutations. *The corrected QT (QTc) missing category involves 110 subjects, 69 of whom died suddenly at a young age without a prior electrocardiogram.

mutations in the transmembrane nonpore, C-terminus, or N-terminus regions (Fig. 2B), and there is no significant difference in event rates among the types of mutation (Fig. 2A), nonmissense mutations, mainly frameshift/nonsense mutations in the C-terminus region, may be an independent risk. Therefore, we further investigated the risk associated with a combination of location and type of mutation.

The cumulative probabilities of first cardiac event for missense mutations within different locations are presented in Figure 2D, and those for mutations located in the α-helical domains within different locations are presented in Figure 2E. Significantly higher event rates were found in subjects with missense mutations (Fig. 2D) and mutations in the α-helical domains (Fig. 2E) located in transmembrane pore region than in those located in any other regions. Among 261 patients with frameshift/nonsense mutations, the event rates were not different by location of mutations (data not shown).

Table 3 Mutation Group by Location, Type, and Topology

Type	Location				
	Transmembrane (S1–S4)	Transmembrane (S5-Loop-S6)	N-Terminus	C-Terminus	Total
Missense					
Topology					
α-helices	31 (12)	170 (63)	25 (9)	44 (16)	270 (100)
β-sheet	—	—	56 (43)	74 (57)	130 (100)
Neither	2 (1)	46 (30)	65 (42)	42 (27)	155 (100)
Total	33 (6)	216 (39)	146 (26)	160 (29)	555 (100)
Frameshift/nonsense					
Topology					
α-helices	5 (10)	41 (84)	3 (6)	—	49 (100)
β-sheet	—	—	4 (100)	—	4 (100)
Neither	6 (3)	2 (1)	56 (27)	144 (69)	208 (100)
Total	11 (4)	43 (17)	63 (24)	144 (55)	261 (100)
Others					
Topology					
α-helices	—	—	—	—	—
β-sheet	—	—	—	7 (100)	7 (100)
Neither	—	—	34 (97)	1 (3)	35 (100)
Total	—	—	34 (81)	8 (19)	42 (100)
Total					
Topology					
α-helices	36 (11)	211 (66)	28 (9)	44 (14)	319 (100)
β-sheet	—	—	60 (43)	81 (57)	141 (100)
Neither	8 (2)	48 (12)	155 (39)	187 (47)	398 (100)
Total	44 (5)	259 (30)	243 (28)	312 (36)	858 (100)

Values are n (%).

The Cox regression analysis by a combination of location and type of mutations for first cardiac events and that for aborted cardiac arrest or LQTS-related sudden cardiac death is presented in Table 4. For patients with missense mutations, the transmembrane pore (S5-loop-S6) and N-terminus regions were a significantly greater risk than the C-terminus region (HR: 2.87 and 1.86, respectively), but the transmembrane nonpore (S1 to S4) region was not (HR: 1.19). However, for nonmissense mutations, these other regions were no longer riskier than the C-terminus (HR: 1.13, 0.77, and 0.46, respectively). Likewise, subjects with nonmissense mutations, mainly frameshift/nonsense mutations, were at significantly higher risk than were subjects with missense mutations in the C-terminus region (HR: 2.00), but that was not the case in other regions. This mutation location-type interaction was significant ($p = 0.008$). However, a mutation topology-type analysis did not reveal a significant interaction ($p = 0.11$). Also, the mutation location-type interaction was not seen for the aborted cardiac arrest or LQTS-related sudden cardiac death end point reported in Table 4.

Among subjects with missense mutations, the transmembrane pore region was a significantly higher risk than were the transmembrane nonpore, N-terminus, or C-terminus regions (not shown HR: 2.42, 1.54, and 2.87, respectively). For subjects with nonmissense mutations, the transmembrane pore region was not a significantly higher risk than were the transmembrane nonpore, N-terminus, or C-terminus regions (HR: 2.47, 1.48, and 1.13, respectively). It is interesting to note that, while not significant, the effect sizes (HRs) of the pore risk stay relatively constant across mutation type except in the case of the C-terminus, further evidence of the location-type interaction.

Discussion

The major findings of the present study from 858 type 2 LQTS subjects with genetically confirmed *KCNH2* mutations derived from 4 LQTS registries are that: 1) there is a significant mutation type-location interaction; specifically, that the relative risk between C-terminus and the regions is different for missense versus nonmissense locations; 2) patients with missense mutations in the transmembrane pore region have significantly higher cardiac event rates than do patients with missense mutations in the N-terminus, transmembrane nonpore, or C-terminus regions; 3) patients with nonmissense mutations were at significantly higher risk than were patients with missense mutations in the C-terminus region; and 4) patients with mutations located in putative α-helical domains have significantly higher cardiac event rates than do patients with mutations in either the β-sheet domains or other uncategorized locations, and these higher event rates are independent of traditional clinical risk factors and of β-blocker therapy. Our data indicate that

Table 4 Cox Regression With Multiple Predictor Variables Including Location and Type of Mutations and Their Interaction for First Cardiac Event and for Aborted Cardiac Arrest/Long QT Syndrome Death

	Hazard Ratio	95% Confidence Interval	p Value
First cardiac event			
1. Mutation location by type			
Transmembrane pore (S5-loop-S6)/C-terminus (reference)			
Missense mutations	2.87	2.03–4.07	<0.001
Nonmissense mutations	1.13	0.65–1.95	0.663
N-terminus/C-terminus (reference)			
Missense mutations	1.86	1.25–2.78	0.002
Nonmissense mutations	0.77	0.50–1.17	0.220
Transmembrane nonpore (S1–S4)/C-terminus (reference)			
Missense mutations	1.19	0.59–2.39	0.632
Nonmissense mutations	0.46	0.18–1.17	0.103
2. Mutation type by location			
Nonmissense/missense (reference)			
C-terminus location	2.00	1.33–3.00	0.001
Other locations (N-terminus, S1–S4, S5-loop-S6)			NS
3. Interaction between mutation location and type*	—	—	0.008
Aborted cardiac arrest/long QT syndrome death			
1. Mutation location by type			
Transmembrane pore (S5-loop-S6)/C-terminus (reference)			
Missense mutations	1.65	0.93–2.91	0.085
Nonmissense mutations	0.57	0.19–1.74	0.324
N-terminus/C-terminus (reference)			
Missense mutations	1.95	0.99–3.83	0.052
Nonmissense mutations	0.80	0.37–1.73	0.575
Transmembrane nonpore (S1–S4)/C-terminus (reference)			
Missense mutations	1.94	0.61–6.20	0.264
Nonmissense mutations	0.55	0.12–2.56	0.446
2. Mutation type by location			
Nonmissense/missense (reference)			
C-terminus location	1.75	0.85–3.61	0.131
Other locations (N-terminus, S1–S4, S5-loop-S6)			NS
3. Interaction between mutation location and type*	—	—	0.208

Note: Items 1, 2, and 3 identify risk factors from the same model. The model adjusted for enrolling site, sex × age, corrected QT, and time-dependent β-blockers as in Table 3. When family members who experienced long QT syndrome-related sudden cardiac death without being genotyped were omitted from the analyses, the hazard ratios, confidence intervals, and p values for location and type of mutation were similar to those values in the above table, but the significance for the interaction between mutation location and type was reduced from p = 0.008 to p = 0.09. *The interaction between mutation location and type measures whether the cardiac event risk for a location relative to the C-terminus varies significantly between missense and nonmissense mutations. The hazard ratio and confidence intervals are not provided for this interaction because the p value is an overall significance level for 3 interaction terms.

NS = not significant.

risk stratification and specific management or treatment by distinct location, coding type, and topology of the channel mutation in addition to classical risk factors such as QTc, sex, or history of prior syncope may be possible in patients with type 2 LQTS, although further studies are definitely required.

A total of 12 forms of congenital LQTS have been reported (2,4,17–20), and clinical studies for genotype-phenotype correlations have been rigorously investigated in the type 1, 2, and 3 LQTS, which constitute >90% of genotyped patients with LQTS (2,21–25). More recently, mutation-location specific differences in the severity of clinical phenotype have been investigated in each genotype (9,11,12,26,27). As to the type 1 LQTS, a large cohort of 600 patients with *KCNQ1* mutations has demonstrated that location and biophysical function of mutations were independent risk factors influencing the clinical course (11). However, the distribution of mutation location as well as the frequency of mutation type are reported to be different in each of 3 major genotypes (9,11,12,26,27). More recently, putative secondary structures of α-helices or β-sheet are reported to have an important role on the channel function in the type 2 LQTS (8). Therefore, a larger cohort of patients having a spectrum of *KCNH2* mutations is required to test the hypothesis that the location, coding type, and topology of mutations would influence the clinical course in the type 2 LQTS.

In contrast to our cohort of 600 type 1 LQTS patients in which the majority of mutations were found in the transmem-

brane region (66.2%) (11), in the present study, mutations in *KCNH2* were more evenly distributed in the N-terminus, the transmembrane domain, and the C-terminus. As to the type of mutation, missense mutations dominated (80.5%), and only 13% of the mutations were frameshift/nonsense mutations in our type 1 LQTS cohort (11). In contrast, missense mutations accounted for 61.7%, and frameshift/nonsense mutations were more frequently observed (35.8%) in this type 2 LQTS cohort. Interestingly, most of the mutations located in the transmembrane pore region were missense mutations (46 of 52, 88.5%) in the present study, a finding concordant with the previous type 2 LQTS cohort by Moss et al. (9) (13 of 14, 92.9%). This indicated that the severe phenotype in patients with mutations located in the transmembrane pore region was probably because missense mutations that are expected to cause dominant negative effects were predominant in this region. However, our type 2 LQTS patients with missense mutations located in the N-terminus, transmembrane nonpore, and C-terminus regions were at significantly less risk than were patients with missense mutations in the transmembrane pore region. These data suggest that location of mutation, in other words, the transmembrane pore region, itself was an independent risk in type 2 LQTS patients with *KCNH2* missense mutation.

Conversely, patients with nonmissense mutations, mainly frameshift/nonsense mutations, were at significantly higher risk than were patients with missense mutations in the C-terminus region, and the event rates in patients with frameshift/nonsense mutations were not different among the transmembrane pore, transmembrane nonpore, N-terminus, and C-terminus regions. Gong et al. (28) recently suggested that most frameshift/nonsense mutations would cause nonsense-mediated decay (NMD), thereby producing less messenger ribonucleic acid from the mutant alleles (28). This potentially would allow for the wild type allele to express more normal channels. Therefore, it is expected that the type 2 LQTS patients with frameshift/nonsense mutation causing NMD would have a mild phenotype. In contrast, the type 2 LQTS patients with frameshift/nonsense mutation without NMD would be expected to have a more severe phenotype because a truncated protein would be produced. Thus, the fact that some frameshift/nonsense mutations show NMD, whereas the other mutations do not, makes the clinical phenotype in the type 2 LQTS patients with frameshift/nonsense mutations more complicated, although this scenario is only a speculation. The present study confirmed the higher risk in patients with nonmissense mutations than in patients with missense mutations in the C-terminus region, suggesting that more careful follow-up is required for type 2 LQTS patients with nonmissense mutations in the C-terminus region.

With regard to the topology of mutation, Anderson et al. (8) recently reported that missense mutations located in a highly ordered structure as α-helices or β-sheet correlated with a class 2 trafficking-deficient phenotype in the type 2 LQTS patients. In the present cohort, mutations located in the α-helical domains were associated with a significantly higher risk compared with mutations in either the β-sheet domains or other uncategorized locations. It is possible that missense mutations in α-helices, where secondary protein structure is thought to be highly ordered, lead to altered secondary and tertiary channel protein structure and abnormal trafficking. This new analysis considering putative secondary structures of mutated channel would be a useful approach in stratifying the risk of cardiac events in patients with LQTS.

β-blockers have long been the first choice of therapy for patients with congenital LQTS (2,29). However, it has been shown in previous studies that the protection that β-blockers provide against cardiac events for type 2 and 3 LQTS patients is somewhat less effective than for type 1 LQTS patients (23,30). A variety of experimental data also support the genotype-specific efficacy of β-blockers for type 1 LQTS (31). In the present study, time-dependent β-blocker use significantly reduced the risk of first cardiac events by 63% ($p < 0.001$), confirming the efficacy of β-blockers as a first line of therapy in patients with type 2 LQTS as well as suggesting more prophylactic use of β-blockers, especially for high-risk patients with type 2 LQTS. However, β-blocker use was associated with less protection (29%) in the prevention of lethal cardiac events compared to first cardiac events (mostly syncope), indicating that additional treatment such as potassium supplement or an implantable cardioverter-defibrillator implantation may be considered in high-risk patients with type 2 LQTS. The patients who have aborted cardiac arrest/sudden death may have a more malignant pathophysiology that is more resistant to β-blockers than are syncopal episodes. We purposely included "ECG missing" in the Cox model so that the β-blocker effect is actually adjusted for subjects with "ECG missing" who probably did not receive β-blockers.

Study limitations. We did not evaluate the risk associated with distinct type of biophysical ion-channel dysfunction (dominant-negative or haplotype insufficient), because only a small percentage of the mutations present within our patient population have been studied extensively in identical cellular expression experiments. There were 60 patients who were not genotyped, and they had an increased risk for events mainly because their fatal events occurred at a young age before they were genotyped. When these patients were excluded from the analysis, the pattern of risk in the missense and nonmissense subgroups remains similar to that of the total population, but the significance of the effect is attenuated because of the reduced number of events.

Reprint requests and correspondence: Dr. Wataru Shimizu, Division of Cardiology, Department of Internal Medicine, National Cardiovascular Center, 5-7-1 Fujishiro-dai, Suita, Osaka 565-8565, Japan. E-mail: wshimizu@hsp.ncvc.go.jp.

REFERENCES

1. Moss AJ, Kass RS. Long QT syndrome: from channels to cardiac arrhythmias. J Clin Invest 2005;115:2018–24.
2. Shimizu W. The long QT syndrome: therapeutic implications of a genetic diagnosis. Cardiovasc Res 2005;67:347–56.